

สเปกโทรสโกปีการทะลุผ่านรอยต่อโลหะปรกติ-ฉนวน-ตัวนำ  
ยวดยิ่งแบบแอนไอโซทรอปิก เอสเวฟ ที่อุณหภูมิอันตะ

นายศรศักดิ์สิทธิ์ บุญมา

วิทยานิพนธ์นี้เป็นส่วนหนึ่งของการศึกษาตามหลักสูตรปริญญาวิทยาศาสตรมหาบัณฑิต  
สาขาวิชาฟิสิกส์  
มหาวิทยาลัยเทคโนโลยีสุรนารี  
ปีการศึกษา 2545  
ISBN 974-533-196-1

**TUNNELING SPECTROSCOPY OF NORMAL  
METAL-INSULATOR-ANISOTROPIC *S*-WAVE  
SUPERCONDUCTOR JUNCTION AT  
FINITE TEMPERATURES**

**Mr. Sonesacksith Bounma**

A Thesis Submitted in Partial Fulfillment of the Requirements  
for the Degree of Master of Sciences in Physics  
Suranaree University of Technology  
Academic Year 2002  
ISBN 974-533-196-1

# TUNNELING SPECTROSCOPY OF NORMAL METAL-INSULATOR-ANISOTROPIC *S*-WAVE SUPERCONDUCTOR JUNCTION AT FINITE TEMPERATURES

Suranaree University of Technology has approved this thesis submitted in partial fulfillment of the requirements for a Master's Degree

## Thesis Examining Committee

---

( Dr. Worasit Uchai )  
Chairman

---

( Dr. Puangratana Pairor )  
Member (Thesis Advisor)

---

( Assoc. Prof. Dr. Samnao Phatisena )  
Member

---

( Dr. Saroj Rujirawat )  
Member

---

( Dr. Sukit Limpijumnong )  
Member

---

(Assoc. Prof. Dr. Tawit Chitsomboon)  
Vice Rector for Academic Affairs

---

(Assoc. Prof. Dr. Prasart Suebka)  
Dean of Institute of Science

ศรศักดิ์สิทธิ์ บุญมา : สเปกโทรสโกปีการทะลุผ่านรอยต่อโลหะปกติ-ฉนวน-ตัวนำยิ่งยวดแบบแอนไอโซทรอปิกเอสเวฟ ที่อุณหภูมิอันตะ

(TUNNELING SPECTROSCOPY OF NORMAL METAL-INSULATOR-ANISOTROPIC S-WAVE SUPERCONDUCTOR JUNCTION AT FINITE TEMPERATURES) อ. ที่ปรึกษา: ดร. พวงรัตน์ ไพเราะ, 42 หน้า.  
ISBN 974-533-196-1

วิทยานิพนธ์นี้เป็นงานวิจัยเกี่ยวกับสเปกโทรสโกปีการทะลุผ่านรอยต่อโลหะปกติ-ฉนวน-ตัวนำยิ่งยวดแบบแอนไอโซทรอปิกเอสเวฟที่อุณหภูมิศูนย์องศาและที่อุณหภูมิอันตะ วิธีการกระเจิงที่เรียกว่ารูปร่างนิยามของ Blonder-Tinkham-Klapwijk ใช้หากระแสและความนำไฟฟ้า ได้แสดงให้เห็นว่าสเปกตรัมความนำขึ้นกับความแรงขวางกัน, ช่องว่างพลังงาน, การวางทิศทางระหว่างหน้า และอุณหภูมิ สเปกตรัมความนำมีลักษณะสำคัญ ซึ่งปรากฏที่ตำแหน่งต่ำสุดของช่องว่างพลังงาน ที่ช่องว่างพลังงานของการกระตุ้นด้วยเวกเตอร์คลื่นที่ขนานกับแนวตั้งฉากระหว่างผิว ที่ช่องว่างพลังงานของการกระตุ้นด้วยเวกเตอร์คลื่นที่ทำมุม  $\frac{\pi}{4}$  กับแนวตั้งฉากระหว่างผิว และที่ค่าสูงสุดของช่องว่างพลังงาน ทั้ง 4 ตำแหน่งนี้ใช้กำหนดค่าช่องว่างพลังงานที่ตำแหน่งต่างๆบนผิวเฟอร์มี ซึ่งเห็นได้ชัดเจนที่อุณหภูมิศูนย์องศาแต่จะขยายกว้างและเลื่อนที่อุณหภูมิอันตะ ดังนั้นการสังเกตค่าเหล่านี้จึงควรกระทำที่อุณหภูมิต่ำกว่า 10 เปรอร์เซ็นต์ของค่าอุณหภูมิเปลี่ยนสถานะ

สาขาวิชาฟิสิกส์

ลายมือชื่อนักศึกษา \_\_\_\_\_

ปีการศึกษา 2545

ลายมือชื่ออาจารย์ที่ปรึกษา \_\_\_\_\_

SONESACKSITH BOUNMA : TUNNELING SPECTROSCOPY OF  
NORMAL METAL-INSULATOR-ANISOTROPIC *S*-WAVE SUPER-  
CONDUCTOR JUNCTION AT FINITE TEMPERATURES.

THESIS ADVISER : DR. PUANGRATANA PAIROR, 42 PP.

ISBN 974-533-196-1

TUNNELING SPECTROSCOPY/ANISOTROPIC *S*-WAVE/CONDUCTANCE  
SPECTRA

The study of the tunneling spectroscopy of a normal metal-insulator-anisotropic *s*-wave superconductor junction at zero and finite temperatures is presented in this thesis. The approach used to obtain the tunneling current and conductance is the scattering method, known as the Blonder-Tinkham-Klapwidjk formalism. It is shown that the conductance spectra depend on the barrier strength, the gap function, the interface orientation and the temperature. There are four main features in the conductance spectra. They occur at the minimum of energy gap, at the energy gap of the excitation with the wave vector parallel to the interface normal, at the energy gap of the excitation with the wave vector making an angle  $\theta = \pi/4$  with the interface normal, and at the maximum energy gap. These four positions can be used to determine the values of the anisotropic *s*-wave gap function at various points on the Fermi surface. At finite temperatures, the four distinct features, clearly seen at zero temperature, are smeared and broadened. Therefore, it is recommended that in order to observe these features presented in this thesis, the experiment should be done at temperatures lower than 10% of the transition temperature.

School of Physics

Student \_\_\_\_\_

Academic Year 2002

Advisor \_\_\_\_\_

# Acknowledgements

First of all I would like to express my sincere thank to my supervisor, Dr. Puangratana Pairor for her guidance, patience and support throughout the course of this study. Though I have been working under her invaluable supervision for a short while, I have had many good academic experiences, which I will always be grateful.

I am also very grateful to all the mentors who have taught, helped, advised and supported me during my study in the School of Physics, Suranaree University of Technology. They are Assoc. Prof. Dr. Samnao Phatisena, Dr. Worasit Uchai, Prof. Dr. Eduard B Manoukian, Asst. Prof. Dr. Yupeng Yan, Dr. Chinorat Kobdaj, Dr. Saroj Rujirawat, Asst. Prof. Dr. Prapun Manyum, Dr. Supagorn Rugmai, Dr. Prayoon Songsiriritthigul and Dr. Sukit Limpijumnong.

I want to express my appreciation to Mr. Jessada Suwannapho, Mr. Seo Mounladok and all physics graduate students at Suranaree University of Technology for their invaluable professional guidance and friendly encouragement.

In addition, I wish to express my special thanks to National University of Laos, Laos Government and Asian Development Bank for the scholarship which enable me to continue my advanced studies at Suranaree University of Technology, Thailand.

Finally, I would like to thank my wife and parents for their love, support, encouragement, and patience throughout the period of producing a dissertation. I cannot thank them enough.

Sonesacksith Bounma

# Contents

	Page
Abstract in Thai	I
Abstract in English	II
Acknowledgements	III
Contents	IV
List of Figures	VI
 Chapter	
<b>I Introduction</b>	<b>1</b>
1.1 Motivation . . . . .	1
1.2 Method and Assumption . . . . .	3
1.3 Outline of Thesis . . . . .	3
<b>II Current and Conductance in the Isotropic Model</b>	<b>5</b>
2.1 Introduction . . . . .	5
2.2 The Reflection and Transmission Probabilities . . . . .	7
2.3 Current and Conductance Formula . . . . .	12
<b>III Tunneling Spectroscopy at Zero Temperature</b>	<b>16</b>
3.1 Introduction . . . . .	16
3.2 Isotropic $s$ -wave Superconductor . . . . .	17
3.3 Anisotropic $s$ -wave Superconductor . . . . .	21

## Contents (Continued)

	<b>Page</b>
<b>IV Tunneling Spectroscopy at Finite Temperatures</b>	<b>31</b>
4.1 Introduction . . . . .	31
4.2 Isotropic <i>s</i> -wave Superconductor . . . . .	32
4.3 Anisotropic <i>s</i> -wave Superconductor . . . . .	34
<b>V Conclusions</b>	<b>36</b>
<b>References</b>	<b>39</b>
<b>Curriculum Vitae</b>	<b>42</b>



# List of Figures

Figure	Page
2.1 The sketch of an NIS junction used in the isotropic model. A potential barrier of the insulating layer is represented by $H\delta(x)$ . $\Delta(k)\Theta(x)$ is the gap function. $\Theta(x)$ is a Heaviside-step function. . .	6
2.2 The sketches of the bulk quasiparticle energies of normal metal (a) and superconductor (b). (c) shows the reflection and transmission processes occurring at the NIS interface. For electron with the wave vector $q^+$ coming from the normal metal, there are two reflected excitations: the Andreev and normal reflected excitations with $q^-$ and $-q^+$ respectively. There are also two transmitted electron-like and hole-like quasiparticle excitations with $k^+$ and $-k^-$ respectively. . .	8
3.1 The sketch of an isotropic Fermi surface of an isotropic $s$ -wave superconductor. $k_F$ is the Fermi wave vector, $\Delta$ is the energy gap of the bulk superconductor. . . . .	17
3.2 The plots of reflection and transmission probabilities at NIS interface as a function of $E/\Delta$ for different values of the barrier strength $Z = 0.0, 0.3, 1.0$ and $1.5$ . $A$ and $B$ are the Andreev and the normal reflection probabilities. $C$ and $D$ are the transmission probabilities of electron-like and hole-like quasiparticle excitation, respectively. . .	18

## List of Figure (Continued)

Figure	Page
3.3	The plots of the normalized current as a function of $(Ve)/\Delta$ , for different the values of the barrier strength $Z = 0.0, 0.6, 1.0, 3.0$ at zero temperature. Note that each curve attain their asymptotic limits (Ohm's law) at high voltage. . . . . 20
3.4	The plots of the normalized conductance of a function $(Ve)/\Delta$ , for various values of $Z$ : 0.0, 0.3, 1.0 and 3.0 at zero temperature. . . . 21
3.5	(a) The sketch of the reflected and transmitted processes in the NIS junction. $\theta$ is the angle between the incident electron beam and the normal of the interface. (b) the Fermi surface ( thick dashed circle) and the gap functions of an anisotropic $s$ -wave geometry in the momentum space. In this figure, $\alpha$ is the angle between the normal of the interface and the $a$ -axis of superconductor. The thin solid curves represent the gap when $\alpha = 0$ , whereas the thin dashed line is the gap when $\alpha \neq 0$ . . . . . 22
3.6	The plots of the gap function of anisotropic $s$ -wave superconductors as a function of an angle $\theta$ for $\alpha = 0$ . (a) $\varepsilon = 1.0$ , (b) $\varepsilon = -1.0$ and (c) $\varepsilon = 0.5$ . . . . . 23
3.7	(a) The sketch of the excitation energy of the superconductor when $\alpha \neq 0$ . Note the inequality in $\Delta_{k+}$ and $\Delta_{k-}$ . The plots of energy gaps as a function of $\theta$ when orientation angle $\alpha = \pi/5$ for (b) $\varepsilon = 1.0$ and (c) $\varepsilon = 0.5$ are shown. The solid curves are for $\Delta_{k+}$ and the dashed curves are for $\Delta_{-k-}$ . . . . . 24

## List of Figure (Continued)

Figure	Page
3.8 The plots of reflection and transmission probabilities of anisotropic $s$ -wave as functions of $E$ for $\theta = \pi/6$ , where $Z = 1.0$ , and $\alpha = 0$ . (a) for $\varepsilon = 1.0$ and (b) for $\varepsilon = 0.5$ . Note that $\Delta_{max} = \Delta_0(1 +  \varepsilon )$ . A and B are the Andreev and the normal reflection probabilities, respectively. C and D are the transmitted probabilities of e-like and h-like quasiparticle excitations, respectively. . . . .	26
3.9 The plots of reflection and transmission probabilities as functions of $E$ when $Z = 1.0$ and $\alpha = \pi/5$ . (a), (b), (c) are for $\varepsilon = 1.0$ at $\theta = 0, \pi/4$ , and $\pi/6$ , respectively and (d), (e), (f) are for $\varepsilon = 0.5$ , at $\theta = 0, \pi/4$ , and $\pi/6$ , respectively. . . . .	27
3.10 The plots of the normalized conductance as a function of $(Ve)/\Delta_{max}$ at zero temperature for $\alpha = 0$ with different the values of barrier strength $Z = 0.0, 0.3, 1.0$ , and $3.0$ . (a) is when $\varepsilon = 1.0$ , and (b) is when $\varepsilon = 0.5$ . . . . .	28
3.11 The plots of the normalized conductance as a function of $(Ve)/\Delta_{max}$ with various the value barrier strength $Z = 0.0, 0.3, 1.0$ and $3.0$ and orientation by angle $\alpha = \pi/5$ . (a) $\varepsilon = 1.0$ , (b) $\varepsilon = 0.5$ . . . . .	29
3.12 The plots of the normalized conductance as a function of $(Ve)/\Delta_{max}$ with various the value of angle $\alpha = 0, \pi/5$ , and $\pi/3$ for $Z = 3.0$ . (a) $\varepsilon = 1.0$ , (b) $\varepsilon = 0.5$ . . . . .	30
4.1 The plots of the normalized conductance as a function of $(Ve)$ at $T/T_C = 0.0, 0.1, 0.2$ , and $0.3$ . (a) for $Z = 0.0$ , and (b) for $Z = 2.5$ .	33
4.2 The plots of the normalized conductance as a function $(Ve)$ at $T/T_C = 0.0, 0.1, 0.2, 0.3$ and $\alpha = 0$ , for (a) $\varepsilon = 1.0$ (b) $\varepsilon = 0.5$ . . .	34
4.3 The plots of the normalized conductance as a function $(Ve)$ at $T/T_C = 0.0, 0.1, 0.2, 0.3$ and $\alpha = \pi/6$ , for (a) $\varepsilon = 1.0$ (b) $\varepsilon = 0.5$ . .	35

# Chapter I

## Introduction

### 1.1 Motivation

The tunneling spectroscopy of a normal metal-insulator-superconductor (NIS) junction is one of most powerful tools used to study the quasiparticle excitations of the superconductor (McMillan, W. L. and Rowell, J. M. 1969; Wolf, E. L. 1985). The physical quantities measured in the tunneling experiment are the current ( $I$ ) that tunnels across the junction and the associated applied voltage ( $V$ ). In addition to the ( $I - V$ ) characteristic of the junction, the conductance, the derivative of current with respect to the applied voltage, is also the quantity of interest. In the tunneling limit, or low transmission limit, the tunneling conductance of the normal metal-superconductor junction is proportional to the density of state (DOS) of the quasiparticle excitations of the superconductor (Giaver, I. 1960; Giaver, I. and Megerle, K. 1961). Therefore, for isotropic  $s$ -wave superconductors, the plot of the conductance as a function of applied voltage in the tunneling limit provides a way of measuring the magnitude of their energy gaps (Tinkham, M. 1996; Duzer, T. V. and Turner, C. W. 1999). The isotropic nature of the energy gap of isotropic  $s$ -wave superconductor results in the independence of the tunneling spectroscopy on the direction, into which the injected current flows with respect to the junction interface. In contrary, the tunneling spectroscopy of anisotropic superconductors would depend on the interface orientation (Kashiyawa, S., *et al.* 1996; Pairor, P. and Walker, M. B. 2002). Thus, the tunneling spectroscopy can be used to study the values of the energy gap of an anisotropic

$s$ -wave superconductor at the different points on the Fermi surface.

Anisotropic  $s$ -wave superconductors are among the anisotropic superconductors. Their gap functions change with the direction in the momentum space. The rare-earth borocarbides, such as  $\text{LuNi}_2\text{B}_2\text{C}$ ,  $\text{YNi}_2\text{B}_2\text{C}$ , and  $\text{MgB}_2$  are the possible examples of anisotropic  $s$ -wave superconductors (Pickett, W. E. and Singh, D. J. 1994; Mun, M-O., *et al.* 1998; Zarestky, J., *et al.* 1999; Civale, L., *et al.* 1999; Buzea, C. and Yamashita, T. 2001; Maki, K., *et al.* 2002). The crystal structures of the borocarbides compounds are tetragonal with the ratio  $c/a$  about 3 (Mun, M-O., *et al.* 1998; Civale, L., *et al.* 1999) while the structure of  $\text{MgB}_2$  is hexagonal with  $c/a > 1$  (Buzea, C. and Yamashita, T. 2001). Because of the large  $c/a$  ratios especially of the borocarbides, these systems can be considered quasi-two-dimensional.

There is still a debate over what is the type of the gap symmetry of these materials. In order to help clarify the gap symmetry of some of these materials, it is useful to study the directional tunneling spectroscopy of two-dimensional superconductors. Because there are a number of experiments indicating that the gap of these materials has anisotropic  $s$ -wave characteristics, it is interesting to examine the tunneling spectroscopy of superconductor with such gap symmetry. The result of this study can be used to compare with the tunneling experimental results and may help eliminate or support this gap symmetry.

In this thesis, the tunneling spectroscopy of tetragonal anisotropic  $s$ -wave superconductors both at zero temperature and at finite temperatures are theoretically studied. For simplicity, throughout this work, the system is assumed to have two-dimensional isotropic Fermi surface. To calculate the current and the conductance of the tunneling junction, the scattering method known as the Blonder-Tinkham-Klapwijk (BTK) formalism (Griffin, A. and Demers, J. 1971; Blonder, G. E., Tinkham, M., and Klapwijk, T. M. 1982) is used. This method has at least one advantage over other methods, like the transfer Hamiltonian method. In the BTK approach, the insulating layer can be set to have arbitrary strength. This freedom provides the ability to study the dependence of the tunneling conductance

spectrum on the strength of the barrier potential as well.

## 1.2 Method and Assumption

One of the theoretical approaches widely used to study the NIS geometry is the scattering method. This method makes use of the Bogoliubov-de Gennes (BdG) equations, which are two-component energy equations and a general form for the quasiparticle wave function of each side of the junction. In a simple case, the wave function of the normal metal is a linear combination of an incoming electron, an Andreev reflected hole, and a normal reflected electron, whereas the wave function of the superconductor is a linear combination of two transmitted quasiparticle excitations: one is electron-like and the other is hole-like. The two wave functions are later on matched at the interface using appropriate boundary conditions in order to evaluate all the reflection and transmission amplitudes. With the associated reflection and transmission probabilities and a suitable Boltzmann equation that explains the non-equilibrium quasiparticle populations in the presence of an applied voltage, the distributions functions of the incoming, reflected and transmitted quasiparticle can be found (Blonder, G. E., Tinkham, M., and Klapwijk, T. M. 1982; Kashiwaya, S., *et al.* 1996). As a result, the electric current across the junction and the tunneling conductance can be expressed in terms of these distribution functions. This method provides an exact expression of the differential conductance and allows one to study it over a wide range of the barrier strength, i.e., from the high transmission or Andreev limit to the low transmission or tunneling limit. This technique is now commonly known as the Blonder-Tinkham-Klapwijk formalism.

## 1.3 Outline of Thesis

This thesis contains the theoretical study of the tunneling spectroscopy of tetragonal anisotropic *s*-wave superconductors at zero and finite temperatures.

Chapter II of this thesis provides the review of the formalism used to obtain the current and conductance of NIS junction at zero and finite temperatures. The model of the junction and all the assumptions used in all the calculations are also described.

In Chapter III, the current and the conductance of NIS junction at differential barrier strengths and angle orientations are studied at zero temperature for both isotropic and anisotropic *s*-wave superconductors. The comparison of the tunneling conductance spectra of both types of superconductors are discussed.

In Chapter IV, the conductance spectra are examined at finite temperatures. Finally, the conclusions are provided in Chapter V.

# Chapter II

## Current and Conductance in the Isotropic Model

### 2.1 Introduction

This chapter mainly provides the review of the method used to obtain the tunneling current and conductance spectrum of a normal metal-insulator-superconductor (NIS) junction in the isotropic model. The assumption used in this model is that the Fermi surfaces of both normal metal and superconductor are isotropic. Since the systems of interest are the borocabides, the crystal structures of which are tetragonal with the ratio of the lattice constants  $c/a \geq 3$ , their Fermi surfaces are taken to be cylindrical, as well as those of the normal metal for simplicity. The shape of the Fermi surface definitely has some effect to the tunneling conductance spectrum; however, it should not affect the main characteristics of the spectrum (Pairor, P. and Walker, M. B. 2002).

The NIS junction is taken to be an infinite system. The insulating layer is taken to have zero width and lies on the  $yz$  plane. The normal metal is in the region where  $x < 0$  and the superconductor fills the  $x > 0$  region. Figure 2.1 shows the geometry of the NIS junction. The insulator is represented by a delta function potential  $V(x) = H\delta(x)$ , where  $H$  is the strength of the potential barrier. The energy gap is assumed to be zero in the normal metal but non-zero and uniform in the superconductor, or  $\Delta(x) = \Delta(k)\Theta(x)$ , where  $\Delta(k)$  is the BCS value of the



energy gap and  $\Theta(x)$  is a Heaviside-step function. The gap can be assumed to be a step-function, since the values of the coherent length  $\xi$  of the Borocarbides are small (Nohara, M., *et al.* 1997; Shulga, S. V., *et al.* 1998; Mortensen, N. A., *et al.* 1999).

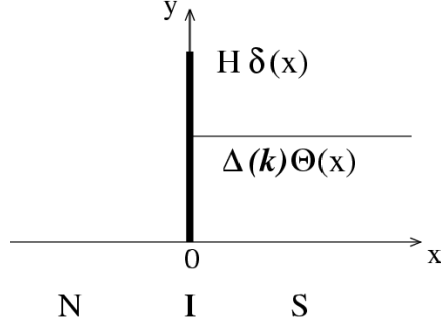


Figure 2.1: The sketch of an NIS junction used in the isotropic model. A potential barrier of the insulating layer is represented by  $H\delta(x)$ .  $\Delta(k)\Theta(x)$  is the gap function.  $\Theta(x)$  is a Heaviside-step function.

The Bogoliubov-de Gennes equations used to describe the junction are, therefore, written as

$$\begin{bmatrix} -\frac{\hbar^2}{2m}\nabla^2 + H\delta(x) - E_F & \Delta(k)\Theta(x) \\ \Delta(k)\Theta(x) & \frac{\hbar^2}{2m}\nabla^2 - H\delta(x) + E_F \end{bmatrix} \psi(r) = E\psi(r), \quad (2.1)$$

where  $E_F$  is the Fermi energy,  $m$  is the electron mass, and  $\psi(r)$  is a two component wave function, or  $\psi(r) = \begin{bmatrix} u(r) \\ v(r) \end{bmatrix}$ , where  $u(r)$  is the electron-like quasiparticle part and  $v(r)$  is the hole-like quasiparticle part.

Because the system is two-dimensional and taken to be in the  $xy$  plane, the bulk excitation energy of the normal metal is obtained as

$$E(q_x, q_y) = \pm \left[ \frac{\hbar^2}{2m}(q_x^2 + q_y^2) - E_F \right], \quad (2.2)$$

where  $q_x, q_y$  are the  $x$  and  $y$  components of the wave vector in the normal state. Note that the energy is always positive and the plus and minus signs correspond to the electron and hole excitation energies, respectively.

Similarly, the bulk excitation energy of the superconductor is

$$E(k_x, k_y) = \sqrt{\xi_k^2 + \Delta_k^2}, \quad (2.3)$$

where  $\xi_k$  is the normal-state excitation energy

$$\xi_k = \frac{\hbar^2}{2m}(k_x^2 + k_y^2) - E_F \quad (2.4)$$

and  $\Delta_k$  is the gap function. The electron-like and hole-like quasiparticle amplitudes are taken to have the form  $u(r) = u_k e^{i\vec{k}\cdot\vec{r}}$  and  $v(r) = v_k e^{i\vec{k}\cdot\vec{r}}$ , where  $u_k$  and  $v_k$  are the BCS electron-like and hole-like quasiparticle excitation amplitudes, respectively. Note that  $u_k$  and  $v_k$  are

$$\begin{aligned} u_k &= \frac{E + \xi_k}{\sqrt{|E + \xi_k|^2 + |\Delta_k|^2}}, \\ v_k &= \frac{\Delta_k}{\sqrt{|E + \xi_k|^2 + |\Delta_k|^2}}, \end{aligned} \quad (2.5)$$

and  $|u_k|^2 + |v_k|^2 = 1$ .

## 2.2 The Reflection and Transmission Probabilities

In order to obtain the current flowing across the junction, the reflection and transmission probabilities are calculated by assuming that an electron incoming from the normal metal side tunnels to the superconducting side. The wave vector of the electron incoming from the normal metal side,  $q^+$ , has the direction that makes an angle  $\theta$  with the  $x$ -axis (see Fig. 2.2(c)).

There exist two types of reflections here. The first one is called Andreev reflection, which has a wave vector  $q^-$ , and the second is the normal reflection with the wave vector  $-q^+$ . Note that while the normal reflection process reduces the number of electrons tunneling across the junction, the Andreev reflection process results in a transport of two electrons across the junction. This is due to the fact that the reflected excitation in the Andreev reflection process is a hole excitation.

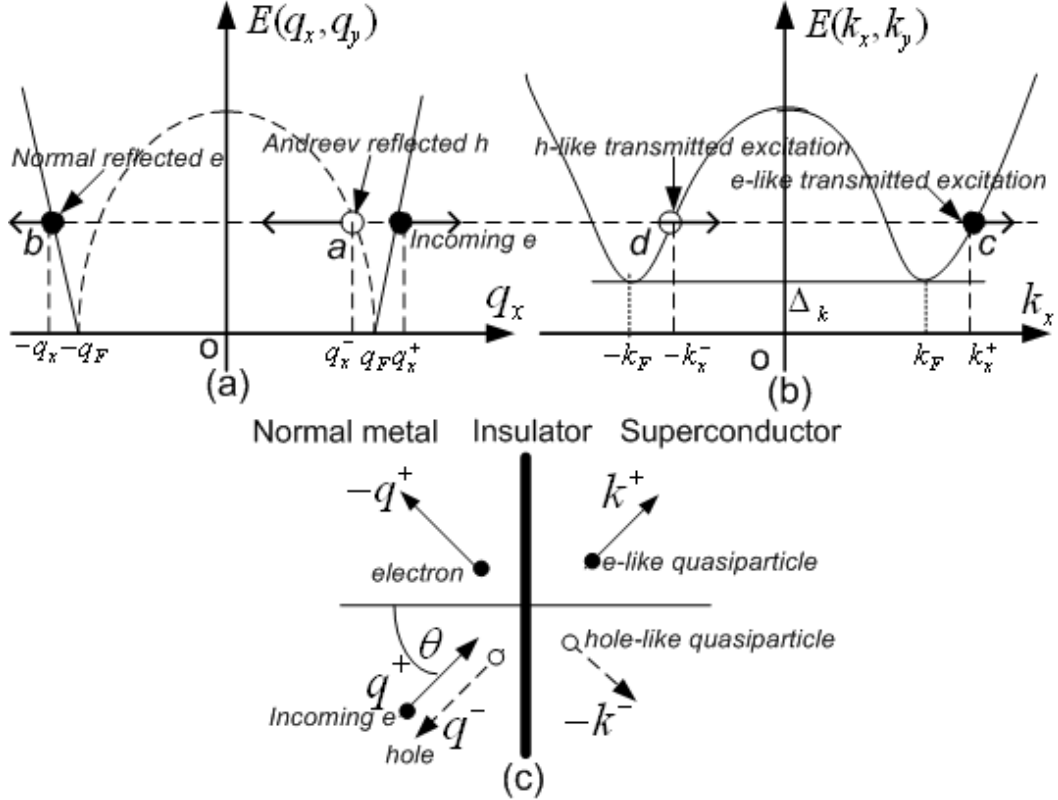


Figure 2.2: The sketches of the bulk quasiparticle energies of normal metal (a) and superconductor (b). (c) shows the reflection and transmission processes occurring at the NIS interface. For electron with the wave vector  $q^+$  coming from the normal metal, there are two reflected excitations: the Andreev and normal reflected excitations with  $q^-$  and  $-q^+$  respectively. There are also two transmitted electron-like and hole-like quasiparticle excitations with  $k^+$  and  $-k^-$  respectively.

There are two transmitted excitations, one is electron-like quasiparticle with

the wave vector  $k^+$  and the other is hole-like quasiparticle with the wave vector  $-k^-$ . Since the system has a translational invariance for the direction parallel to the interface, the wave vector components along this direction are conserved, and the wave function of an incoming electron on the normal side can be written as

$$\psi_N(x < 0, y) = \psi_I + \psi_{R(h)} + \psi_{R(e)},$$

$$\psi_N(x < 0, y) = \left( \begin{bmatrix} 1 \\ 0 \end{bmatrix} e^{iq_x^+ x} + a \begin{bmatrix} 0 \\ 1 \end{bmatrix} e^{iq_x^- x} + b \begin{bmatrix} 1 \\ 0 \end{bmatrix} e^{-iq_x^+ x} \right) e^{ik_y y}, \quad (2.6)$$

where  $a, b$  are the Andreev and normal reflection amplitudes respectively and  $q_x^\pm$  satisfy the energy equation Eq. (2.2) for electron and hole excitations. In Eq. (2.6), the first term is the incident electron, the second is the Andreev reflected hole, and the third is normal reflected electron. In the superconductor, the wave function is the sum of the two transmitted excitations

$$\psi_S(x > 0, y) = \psi_{T(e)} + \psi_{T(h)},$$

$$\psi_S(x > 0, y) = \left( c \begin{bmatrix} u_{k^+} \\ v_{k^+} \end{bmatrix} e^{ik_x^+ x} + d \begin{bmatrix} u_{-k^-} \\ v_{-k^-} \end{bmatrix} e^{-ik_x^- x} \right) e^{ik_y y}, \quad (2.7)$$

where  $c, d$  are the two transmission amplitudes, and  $k_x^\pm$  satisfy the energy equation Eq. (2.3) at the same  $k_y$ . In Eq. (2.7) the first term represents the transmission of the electron-like quasiparticle and the second term represents the transmission of the hole-like quasiparticle crossing the Fermi surface.

The amplitudes  $a, b, c$  and  $d$  are calculated by using the matching conditions at the interface, which are

$$\begin{aligned} \psi_S(x, y) \Big|_{x=0^+} &= \psi_N(x, y) \Big|_{x=0^-} = \psi(0, y), \\ \frac{d}{dx} \psi_S(x, y) \Big|_{x=0^+} - \frac{d}{dx} \psi_N(x, y) \Big|_{x=0^-} &= 2k_F Z \psi(0, y), \end{aligned} \quad (2.8)$$

where  $Z = \frac{mH}{k_F \hbar^2}$  is a dimensionless parameter to represent the insulating barrier strength of the junction ( $H$  is the strength of the potential barrier).

Because the energy range of interest is of the same order as the energy gap which is usually a few orders of magnitude smaller than the Fermi energy, the wave vectors of the quasiparticles will be approximately  $q_x^+ \approx q_x^- \approx q_F \cos \theta$  and  $k_x^+ \approx k_x^- \approx k_F \cos \theta$ , where  $\theta$  is angle between direction of the wave vector and the  $x$ -axis.

Let the ratio of the two Fermi wave numbers  $\lambda = q_F/k_F$ . Eq. (2.8) can be written as

$$\begin{bmatrix} 0 & 1 & -u_{k^+} & -u_{-k^-} \\ 1 & 0 & -v_{k^+} & -v_{-k^-} \\ 0 & (\lambda + \frac{2iZ}{\cos \theta}) & u_{k^+} & -u_{-k^-} \\ -(\lambda - \frac{2iZ}{\cos \theta}) & 0 & v_{k^+} & -v_{-k^-} \end{bmatrix} \begin{bmatrix} a \\ b \\ c \\ d \end{bmatrix} = \begin{bmatrix} -1 \\ 0 \\ (\lambda - \frac{2iZ}{\cos \theta}) \\ 0 \end{bmatrix}, \quad (2.9)$$

the solution of which is as follows

$$a(E, \theta) = \frac{4v_{k^+}v_{-k^-} - \lambda}{u_{k^+}v_{-k^-}(4Z^2 \sec^2 \theta + (1 + \lambda)^2) - u_{-k^-}v_{k^+}(4Z^2 \sec^2 \theta + (\lambda - 1)^2)},$$

$$b(E, \theta) = \frac{(u_{-k^-}v_{k^+} - u_{k^+}v_{-k^-})(1 + 4Z^2 \sec^2 \theta + 4iZ\lambda \sec \theta - \lambda^2)}{u_{k^+}v_{-k^-}(4Z^2 \sec^2 \theta + (1 + \lambda)^2) - u_{-k^-}v_{k^+}(4Z^2 \sec^2 \theta + (\lambda - 1)^2)},$$

$$c(E, \theta) = \frac{2v_{-k^-} - \lambda \sec \theta((1 + \lambda) \cos \theta - 2iZ)}{u_{k^+}v_{-k^-}(4Z^2 \sec^2 \theta + (1 + \lambda)^2) - u_{-k^-}v_{k^+}(4Z^2 \sec^2 \theta + (\lambda - 1)^2)},$$

$$d(E, \theta) = \frac{2v_{k^+} + \lambda \sec \theta(2iZ + (1 - \lambda) \cos \theta)}{u_{k^+}v_{-k^-}(4Z^2 \sec^2 \theta + (1 + \lambda)^2) - u_{-k^-}v_{k^+}(4Z^2 \sec^2 \theta + (\lambda - 1)^2)}. \quad (2.10)$$

The Andreev reflection probability  $A(E, \theta)$  is equal to the magnitude of the ratio between the current density due to the reflected hole and the current density due to the incident electron, i.e.,

$$A(E, \theta) = \left| \frac{J_{R(h)}}{J_{I(e)}} \right| = \left| \frac{n_{R(h)}v_{R(h)}}{n_{I(e)}v_{I(e)}} \right| ,$$

where  $n_{R(h)} = |\psi_{R(h)}|^2$  and  $v_{R(h)}$  is group velocity of the reflected hole. Similarly,  $n_{I(e)} = |\psi_{I(e)}|^2$  and  $v_{I(e)}$  is group velocity of the incident electron. The Andreev reflection probability is therefore equal to

$$A(E, \theta) = |a(E, \theta)|^2 \left| \frac{q_x^+}{q_x^-} \right| \approx |a(E, \theta)|^2 . \quad (2.11)$$

By the same token, the normal reflection probability of the junction  $B(E, \theta)$  is

$$B(E, \theta) = \left| \frac{J_{R(e)}}{J_{I(e)}} \right| = \left| \frac{n_{R(e)}v_{R(e)}}{n_{I(e)}v_{I(e)}} \right| \approx |b(E, \theta)|^2 , \quad (2.12)$$

where  $n_{R(e)} = |\psi_{R(e)}|^2$  and  $v_{R(e)}$  is group velocity of the reflected electron. The transmission probability of the electron-like quasiparticle through the interface of the junction  $C(E, \theta)$  is equal to

$$\begin{aligned} C(E, \theta) &= \left| \frac{J_{T(e)}}{J_{I(e)}} \right| = \left| \frac{n_{T(e)}v_{T(e)}}{n_{I(e)}v_{I(e)}} \right| = |c(E, \theta)|^2 (|u_{k^+}|^2 - |v_{k^+}|^2) \left| \frac{k_x^+}{q_x^+} \right| \\ &\Rightarrow C(E, \theta) \approx |c(E, \theta)|^2 (|u_{k^+}|^2 - |v_{k^+}|^2) \frac{1}{\lambda} . \end{aligned} \quad (2.13)$$

The other transmission probability of the hole-like quasiparticle  $D(E, \theta)$  is

$$\begin{aligned} D(E, \theta) &= \left| \frac{J_{T(h)}}{J_{I(e)}} \right| = \left| \frac{n_{T(h)}v_{T(h)}}{n_{I(e)}v_{I(e)}} \right| = |d(E, \theta)|^2 (|u_{-k^-}|^2 - |v_{-k^-}|^2) \left| \frac{k_x^-}{q_x^+} \right| \\ &\Rightarrow D(E, \theta) \approx |d(E, \theta)|^2 (|u_{-k^-}|^2 - |v_{-k^-}|^2) \frac{1}{\lambda} . \end{aligned} \quad (2.14)$$

Because there is no lost in the number of particles,

$$A(E, \theta) + B(E, \theta) + C(E, \theta) + D(E, \theta) = 1. \quad (2.15)$$

In the case where the superconductor becomes normal, or the system becomes an NIN junction, the Andreev reflection probability  $A(E, \theta) = 0$ , and so is the hole-like transmission probability  $D(E, \theta)$ . Eq.(2.15) would become  $B(E, \theta) + C(E, \theta) = 1$ . Also, the amplitude of reflection and transmission  $b$  and  $c$  for this system would be

$$\begin{aligned} b(\theta) &= -1 + \frac{2\lambda}{(1 + \lambda) + 2iZ \sec\theta}, \\ c(\theta) &= \frac{2\lambda}{(1 + \lambda) + 2iZ \sec\theta}. \end{aligned} \quad (2.16)$$

Thus, the reflection and transmission probabilities in the case of an NIN junction are

$$B(\theta) = \frac{(\lambda - 1)^2 + 4Z^2 \sec^2\theta}{(1 + \lambda)^2 + 4Z^2 \sec^2\theta}, \quad (2.17)$$

$$C(\theta) = \frac{4\lambda}{(1 + \lambda)^2 + 4Z^2 \sec^2\theta}. \quad (2.18)$$

Note that they do not depend on the energy  $E$ .

## 2.3 Current and Conductance Formula

In general, the current flowing in the  $+x$  direction (positive group velocity) across the junction is given by

$$I = \sum_k n_k v_k e, \quad (2.19)$$

where  $n_k$  is number of electron tunneling through the junction, the summation is over all the states with positive  $v_k = \frac{1}{\hbar} \frac{dE}{dk}$ , which is the group velocities, and  $e$  is the electron charge. The number  $n_k$  can be written in terms of

the reflection and transmission probabilities and the Fermi distribution function  $f(E)=[1+\exp(E/k_B T)]^{-1}$  as

$$n_k = [1 + A(E, \theta) - B(E, \theta)]f(E).$$

The Fermi distribution function  $f(E)$  describing the probability of a state with energy  $E$  being occupied at a finite temperature  $T$ ,  $k_B$  is the Boltzmann constant. The value  $[1 + A(E, \theta) - B(E, \theta)]$  can be interpreted as the number of an electron getting transmitted from the normal to the superconducting region per one incident electron. At equilibrium (no applied voltages), the current flowing from the normal metal to superconductor is the same as the current flowing from the superconductor to the normal metal. If there is a non-zero applied voltage, the two currents will be different and cause the net current across the junction. The current flowing across the junction with the applied voltage  $V$  from normal metal to the superconductor can be written as

$$I_{N \rightarrow S} = \frac{L^2 e}{4\pi^2 \hbar} \int_{-\infty}^{+\infty} \int_{-\infty}^{+\infty} dk_y dE [1 + A(E, \theta) - B(E, \theta)] f(E - Ve),$$

while, the current flowing from superconductor to the normal metal can be written as

$$I_{S \rightarrow N} = \frac{L^2 e}{4\pi^2 \hbar} \int_{-\infty}^{+\infty} \int_{-\infty}^{+\infty} dk_y dE [1 + A(E, \theta) - B(E, \theta)] f(E).$$

Thus, the net current crossing the junction is

$$I(Ve, \theta) = I_{N \rightarrow S} - I_{S \rightarrow N}$$

$$\Rightarrow I(Ve, \theta) = \frac{L^2 e}{4\pi^2 \hbar} \int_{-\infty}^{+\infty} \int_{-\infty}^{+\infty} dk_y dE [1 + A(E, \theta) - B(E, \theta)] [f(E - Ve) - f(E)], \quad (2.20)$$



where  $L^2$  is the size of the system,  $(Ve)$  is the resulting difference in the chemical potential across the junction. Because  $k_y = k_F \sin\theta \Rightarrow dk_y = k_F \cos\theta d\theta$ , the net current across the NIS junction can be rewritten as

$$I_{NIS}(Ve, \theta) = \frac{eL^2 k_F}{4\pi^2 \hbar} \int_{-\pi/2}^{+\pi/2} d\theta \cos\theta \int_{-\infty}^{+\infty} dE T_{NIS} [f(E - Ve) - f(E)], \quad (2.21)$$

where  $T_{NIS} = [1 + A(E, \theta) - B(E, \theta)]$ . For the NIN junction  $A(E, \theta) = 0 \Rightarrow T_{NIN} = [1 - B(\theta)] = \frac{4\lambda}{(1+\lambda)^2 + 4Z^2 \sec^2\theta}$  the net current crossing the NIN junction becomes

$$I_{NIN}(Ve, \theta) = \frac{eL^2 k_F}{4\pi^2 \hbar} \int_{-\pi/2}^{+\pi/2} d\theta \cos\theta \int_{-\infty}^{+\infty} dE T_{NIN} [f(E - Ve) - f(E)]. \quad (2.22)$$

Define the normalized current of the junction as the ratio of the NIS current to the NIN current:

$$I(Ve, \theta) = \frac{I_{NIS}}{I_{NIN}} = \frac{\int_{-\pi/2}^{+\pi/2} d\theta \cos\theta \int_{-\infty}^{+\infty} dE T_{NIS} [f(E - Ve) - f(E)]}{\int_{-\pi/2}^{+\pi/2} d\theta \cos\theta \int_{-\infty}^{+\infty} dE T_{NIN} [f(E - Ve) - f(E)]}. \quad (2.23)$$

The conductance of the junction is the derivative of the current with respect to the applied voltage across the junction. The conductance of the NIS junction is

$$G_{NIS}(Ve, \theta) = \frac{dI_{NIS}(Ve, \theta)}{dV},$$

and for the NIN junction the conductance is

$$G_{NIN}(Ve, \theta) = \frac{dI_{NIN}(Ve, \theta)}{dV}.$$

The normalized conductance of the junction is defined by the ratio of  $G_{NIS}$  to

$G_{NIN}$ :

$$G(Ve, \theta) = \frac{G_{NIS}}{G_{NIN}} = \frac{\int_{-\pi/2}^{+\pi/2} d\theta \cos\theta \int_{-\infty}^{+\infty} dET_{NIS} \frac{\partial}{\partial V} f(E - Ve)}{\int_{-\pi/2}^{+\pi/2} d\theta \cos\theta \int_{-\infty}^{+\infty} dET_{NIN} \frac{\partial}{\partial V} f(E - Ve)}. \quad (2.24)$$

At zero temperature Eq.(2.24) is reduced to

$$G(Ve, \theta) = \frac{G_{NIS}}{G_{NIN}} = \frac{\int_{-\pi/2}^{+\pi/2} d\theta \cos\theta \int_{-\infty}^{+\infty} dET_{NIS}}{\int_{-\pi/2}^{+\pi/2} d\theta \cos\theta \int_{-\infty}^{+\infty} dET_{NIN}}. \quad (2.25)$$

The normalized current and normalized conductance formula in this chapter are used to obtain the current and conductance spectra in the next chapters.

# Chapter III

## Tunneling Spectroscopy at Zero Temperature

### 3.1 Introduction

In this chapter the current and conductance for the isotropic and anisotropic  $s$ -wave superconductor at zero temperature are presented. The effects of the crystal orientation of the superconductor and the barrier strength are examined in details. For simplicity, the magnitudes of the Fermi wave vectors of both normal metal and superconductor are taken to be the same, i.e.,  $\lambda = 1$ . It is found that difference in the magnitude of the two Fermi wave vectors affects the tunneling spectroscopy in the same way as an increase in the barrier strength.

The normalized current and the normalized conductance can be calculated from

$$I(Ve, \theta) = \frac{I_{NIS}}{I_{NIN}} = \frac{\int_{-\pi/2}^{+\pi/2} d\theta \cos\theta \int_{-\infty}^{+\infty} dE T_{NIS}}{\int_{-\pi/2}^{+\pi/2} d\theta \cos\theta \int_{-\infty}^{+\infty} dE T_{NIN}} \quad (3.1)$$

and

$$G(Ve, \theta) = \frac{G_{NIS}}{G_{NIN}} = \frac{\int_{-\pi/2}^{+\pi/2} d\theta \cos\theta T_{NIS}}{\int_{-\pi/2}^{+\pi/2} d\theta \cos\theta T_{NIN}}, \quad (3.2)$$

where

$$T_{NIS} = [1 + A(E, \theta) - B(E, \theta)]$$

and

$$T_{NIN} = [1 - B(\theta)] = \frac{1}{1 + Z^2 \sec^2 \theta}.$$

$T_{NIS}$  is the transmission probability across the insulating barrier when the system is NIS junction and  $T_{NIN}$  is the transmission probability across the insulating barrier when both sides of the junction are normal metal. Both  $T_{NIN}$  and  $T_{NIS}$  can be considered as a number of electrons crossing NIN and NIS junctions for each incident electron respectively.

### 3.2 Isotropic $s$ -wave Superconductor

The gaps of an isotropic  $s$ -wave superconductor are shown in Fig. 3.1. The energy gap is the same at all points on the Fermi surface. Therefore, the energy gaps of both transmitted excitations are the same, i.e.,  $\Delta_{k+} = \Delta_{-k-}$ . This means there are simple relations between the BCS parameters  $u_{k\pm}$  and  $v_{k\pm}$ , i.e.,  $u_{k+} = v_{-k-}$  and  $u_{-k-} = v_{k+}$ .

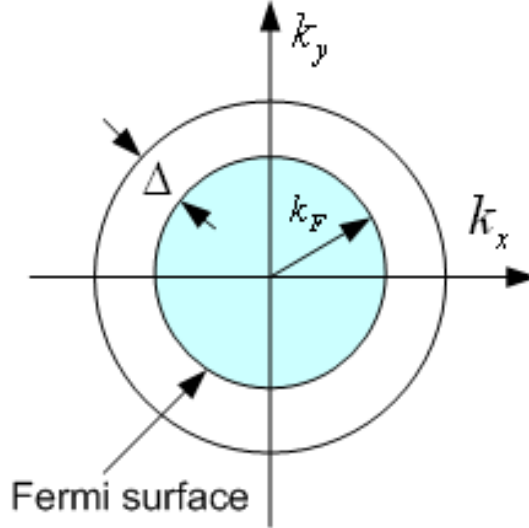


Figure 3.1: The sketch of an isotropic Fermi surface of an isotropic  $s$ -wave superconductor.  $k_F$  is the Fermi wave vector,  $\Delta$  is the energy gap of the bulk superconductor.

The reflection and transmission probabilities of the junction can be calculated from Eqs. (2.11)-(2.14). The result of the calculations for the values of four coefficients  $A(E)$ ,  $B(E)$ ,  $C(E)$ , and  $D(E)$  as functions of energy and barrier strength are shown in Fig 3.2.

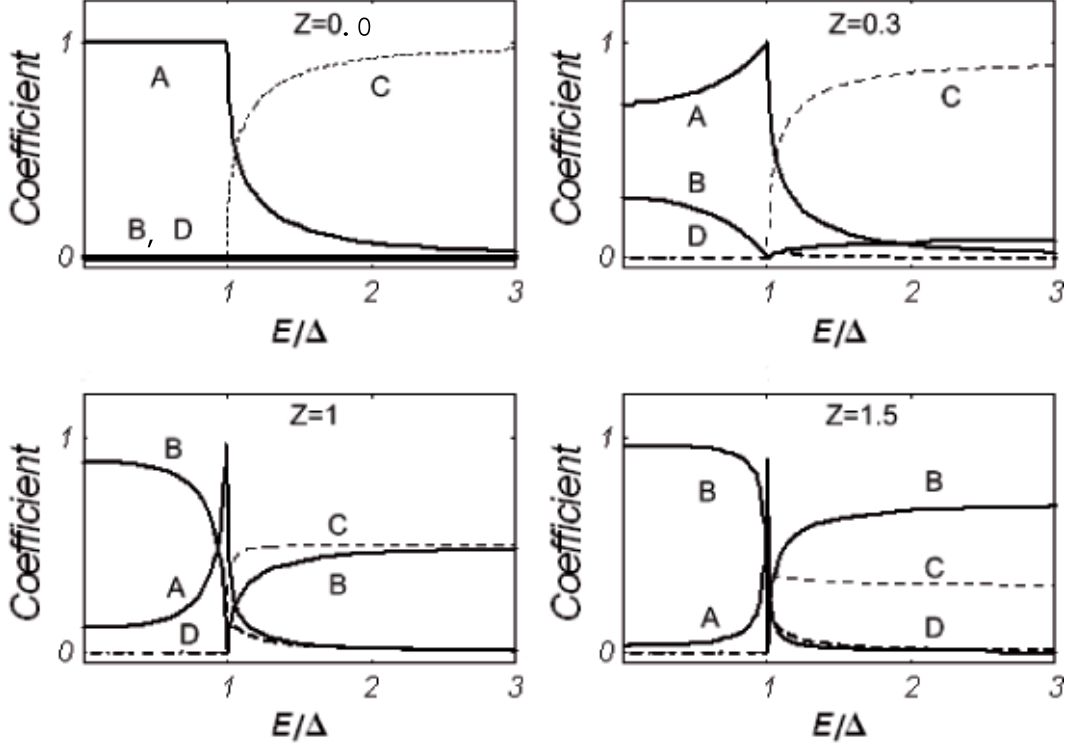


Figure 3.2: The plots of reflection and transmission probabilities at NIS interface as a function of  $E/\Delta$  for different values of the barrier strength  $Z = 0.0, 0.3, 1.0$  and  $1.5$ .  $A$  and  $B$  are the Andreev and the normal reflection probabilities.  $C$  and  $D$  are the transmission probabilities of electron-like and hole-like quasiparticle excitation, respectively.

The reflection and transmission coefficients are plotted as a function of  $E/\Delta$  for different the values of the barrier strength:  $Z = 0.0, 0.3, 1.0$ , and  $1.5$ .

When  $E < \Delta$ , there are no transmitted quasiparticle excitations  $C(E) = D(E) = 0$  for all values of barrier strength. If the barrier strength  $Z$  is weak, the Andreev reflection probability dominates. If the barrier strength  $Z$  is strong, the normal reflection probability is high.

When  $E > \Delta$ , the transmission probability without branch crossing dominates for weak barriers. For strong barriers, the normal reflection probability is high.

In the case of  $E = \Delta$ , one should note that  $A = 1$  and  $B = C = D = 0$ , independent of  $Z$ .

When both sides of interface are normal metals the Andreev reflection probability  $A(E) = 0$  and  $T_{NIN} = 1 - B(E) = C(E) = (1 + Z^2)^{-1}$ . The current across the junction reduces to the simple form

$$I_{NIN} = \frac{eL^2k_F}{4\pi^2\hbar(1 + Z^2)}V = G_{NIN}V ,$$

which is Ohmic;  $G_{NIN}$  is the NIN conductance, which is a constant. Therefore, the normalized current across the junction can be written as

$$I(Ve) = \frac{(1 + Z^2)}{V} \int_0^{(Ve)} dE [1 + A(E) - B(E)]. \quad (3.3)$$

Figure 3.3 shows the plots of the normalized currents across the junction as a function of  $(Ve)/\Delta$  with different values of the barrier strength  $Z$ . In this figure, in the low transmission limit (large  $Z$ ), there is no tunneling current until  $|V|e > \Delta$ , and the current reaches the Ohm's law limit when the applied voltage is large. In the Andreev limit, there is current flowing across the junction even when  $(Ve) < \Delta$ . This is due to the Andreev reflection process, which causes two electrons to tunnel across the junction.

The tunneling normalized conductance as a function of voltage and the barrier strength of the junction is given by

$$G(Ve) = (1 + Z^2)[1 + A(Ve) - B(Ve)]. \quad (3.4)$$

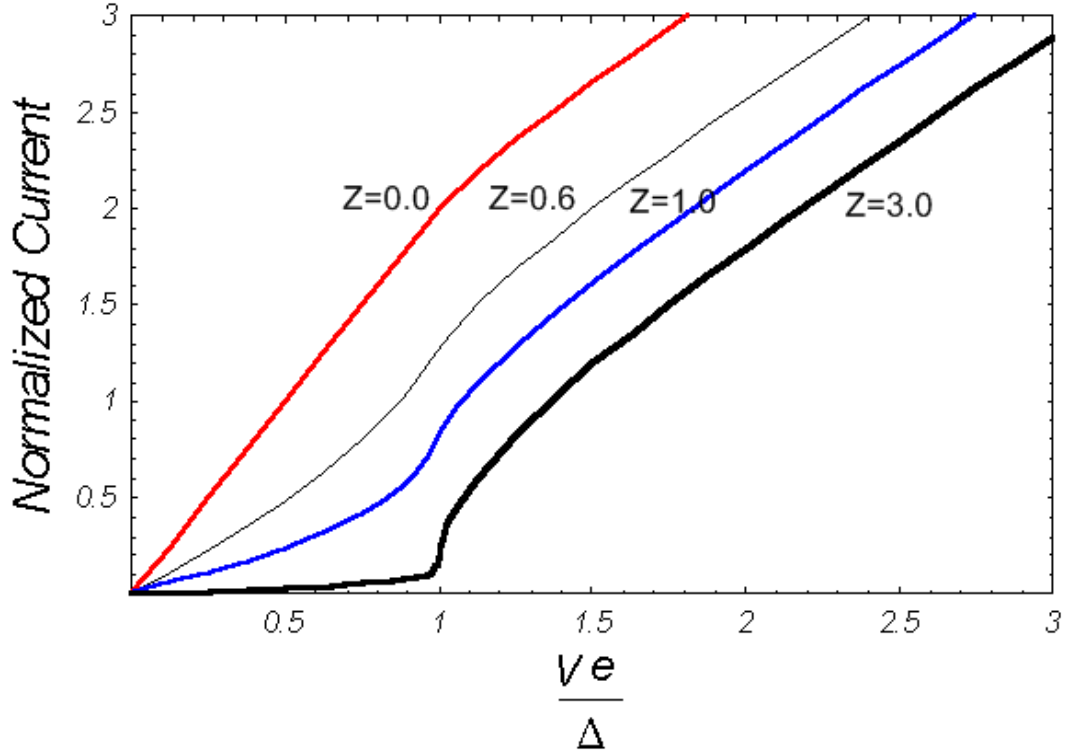


Figure 3.3: The plots of the normalized current as a function of  $(Ve)/\Delta$ , for different the values of the barrier strength  $Z = 0.0, 0.6, 1.0, 3.0$  at zero temperature. Note that each curve attain their asymptotic limits (Ohm's law) at high voltage.

Figure 3.4 shows the plots of tunneling normalized conductance as a function of  $(Ve)/\Delta$  at zero temperature for different values of the barrier strength. It should be pointed out that when  $Z = 0.0$ , and  $(Ve) < \Delta$ , the normalized conductance  $G(Ve) = 2$ , indicating two electrons are transferred across the boundary. When the barrier strength is increased, the normalized conductance is small for  $(Ve) < \Delta$ . When  $(Ve) = \Delta$ , the normalized conductance is peaked.

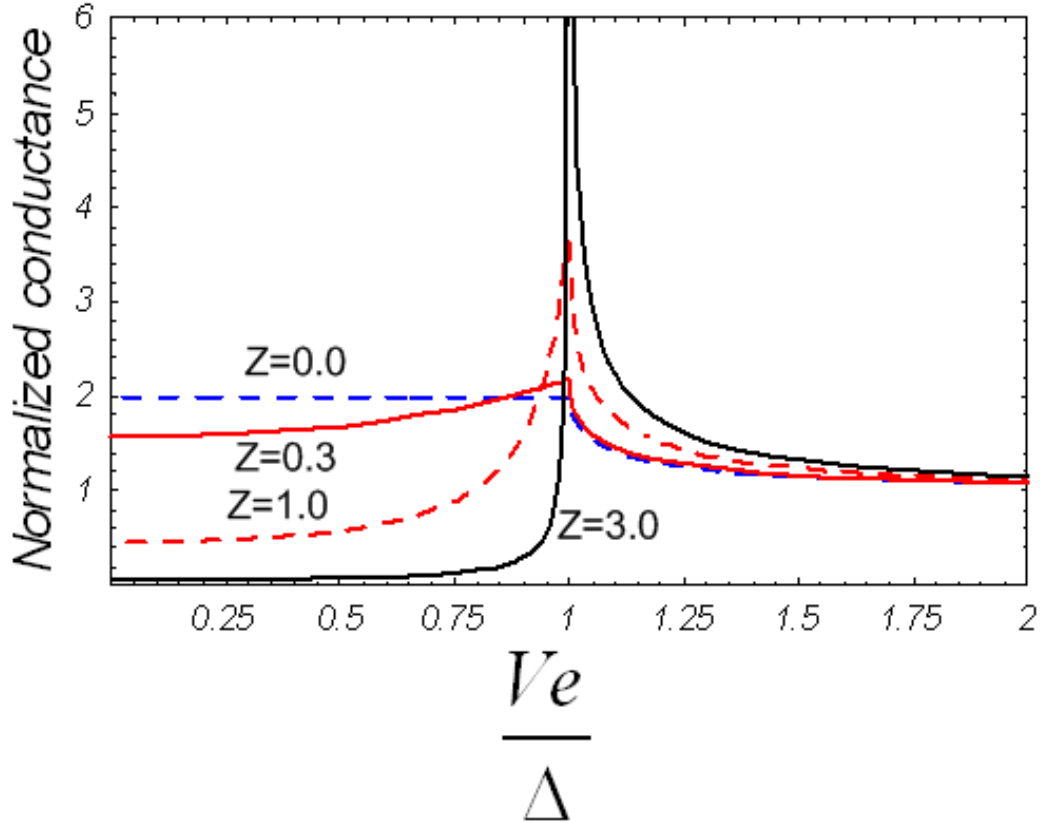


Figure 3.4: The plots of the normalized conductance of a function  $(Ve)/\Delta$ , for various values of  $Z$ : 0.0, 0.3, 1.0 and 3.0 at zero temperature.

### 3.3 Anisotropic $s$ -wave Superconductor

Anisotropic  $s$ -wave superconductors are the superconductors with the gap functions that change their values with the direction in the momentum space. The rare-earth borocarbides, such as  $\text{LuNi}_2\text{B}_2\text{C}$ ,  $\text{YNi}_2\text{B}_2\text{C}$ , and  $\text{MgB}_2$  are the possible examples of anisotropic  $s$ -wave superconductors. These systems can be considered quasi two-dimensional, because of their large  $c/a$  ratio.

In general, the energy gap of anisotropic  $s$ -wave superconductor varies with the angle with respect to a crystal axis. Thus, the tunneling spectroscopy of anisotropic superconductor depends on the crystallographic orientation of the superconductor. Figure 3.5(b) shows an example of the energy gap when the  $a$ -axis is on the  $x$ -axis (thin solid curve) and when the  $a$ -axis makes an angle  $\alpha$  with the



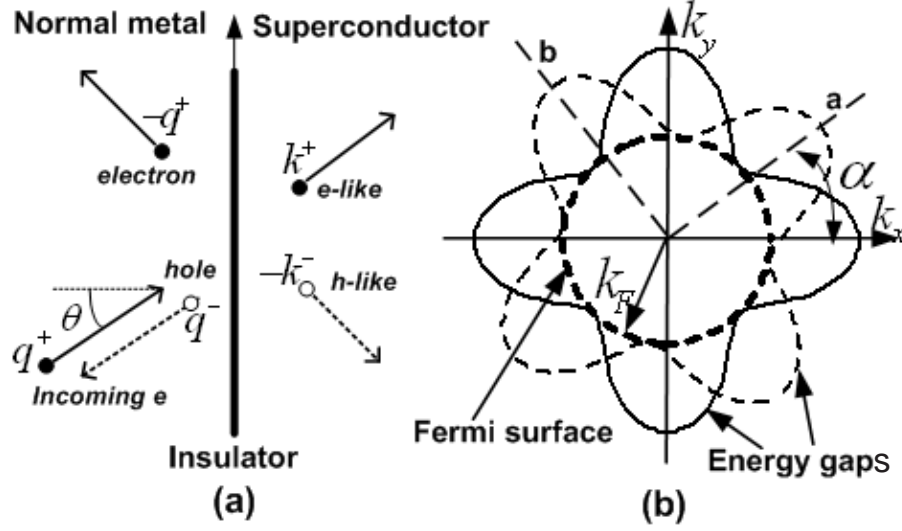


Figure 3.5: (a) The sketch of the reflected and transmitted processes in the NIS junction.  $\theta$  is the angle between the incident electron beam and the normal of the interface. (b) the Fermi surface ( thick dashed circle) and the gap functions of an anisotropic  $s$ -wave geometry in the momentum space. In this figure,  $\alpha$  is the angle between the normal of the interface and the  $a$ -axis of superconductor. The thin solid curves represent the gap when  $\alpha = 0$ , whereas the thin dashed line is the gap when  $\alpha \neq 0$ .

$x$ -axis (thin dashed curve).

The wave vectors of both sides are taken to be  $q_x^+ \approx q_x^- \approx q_F \cos \theta$ ,  $k_x^+ \approx k_x^- \approx k_F \cos \theta$ , and  $q_F = k_F$ . For an anisotropic  $s$ -wave superconductor, the electron-like quasiparticle and the hole-like quasiparticle thus have different effective pair potentials which are  $\Delta_{k^+}$  and  $\Delta_{k^-}$ , respectively:

$$\Delta_{k^\pm} \equiv \Delta(1 + \varepsilon \cos[4(\theta \mp \alpha)]), \quad (3.5)$$

where  $\varepsilon$  is the parameter of the gap function. Different values of  $\varepsilon$  give different shapes of the gap function in the momentum space,  $\alpha$  is an angle between  $a$ -axis and the  $x$ -axis, and  $\theta$  is an angle between the direction of a Fermi wave vector and the  $x$ -axis.  $\Delta_{k^+} = \Delta_{k^-}$  only when  $\alpha = 0$  and  $\frac{\pi}{4}$ . The plots of the energy gap for

$\alpha = 0$  as a function of an angle  $\theta$  with different parameter of the gap function  $\varepsilon$  are shown in Fig. 3.6.

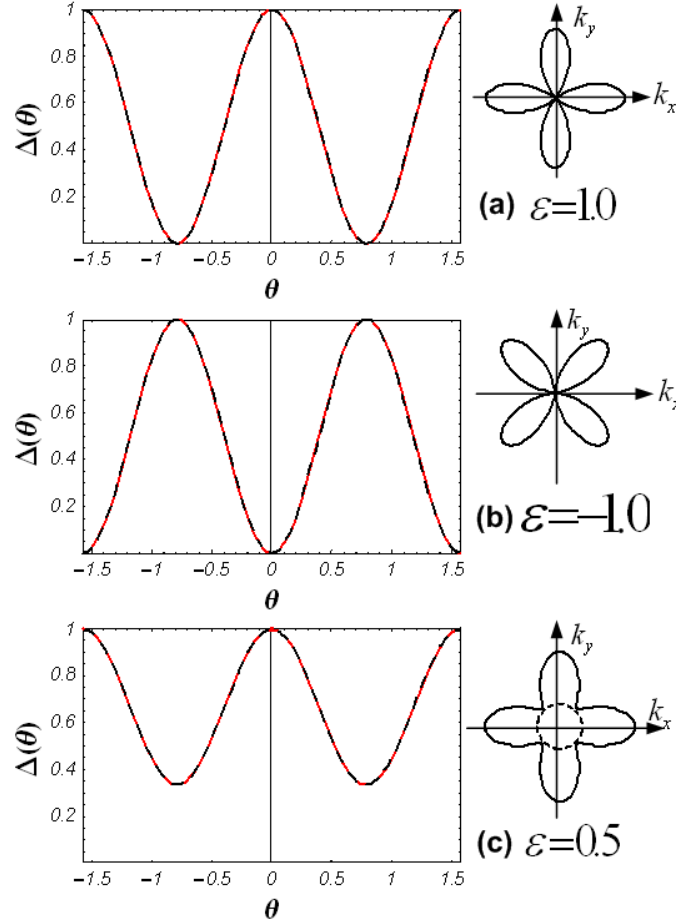


Figure 3.6: The plots of the gap function of anisotropic  $s$ -wave superconductors as a function of an angle  $\theta$  for  $\alpha = 0$ . (a)  $\varepsilon = 1.0$ , (b)  $\varepsilon = -1.0$  and (c)  $\varepsilon = 0.5$ .

When  $\alpha \neq 0$ , the energy gap of both transmitted excitations are different. Figure 3.7 shows the plots of the energy gaps as a function of  $\theta$  for  $\alpha = \pi/5$  in two cases:  $\varepsilon = 1.0$  (b), and  $\varepsilon = 0.5$  (c). In each case, the energy gap of the electron-like excitation  $\Delta_{k+}$  is the solid curve and that of the hole-like  $\Delta_{-k-}$  is the dashed curve. As can be seen, the magnitudes of  $\Delta_{k+}$  and  $\Delta_{-k-}$  are different for the same the incident angle  $\theta$  (except at  $\theta = 0, \pi/4$ ).

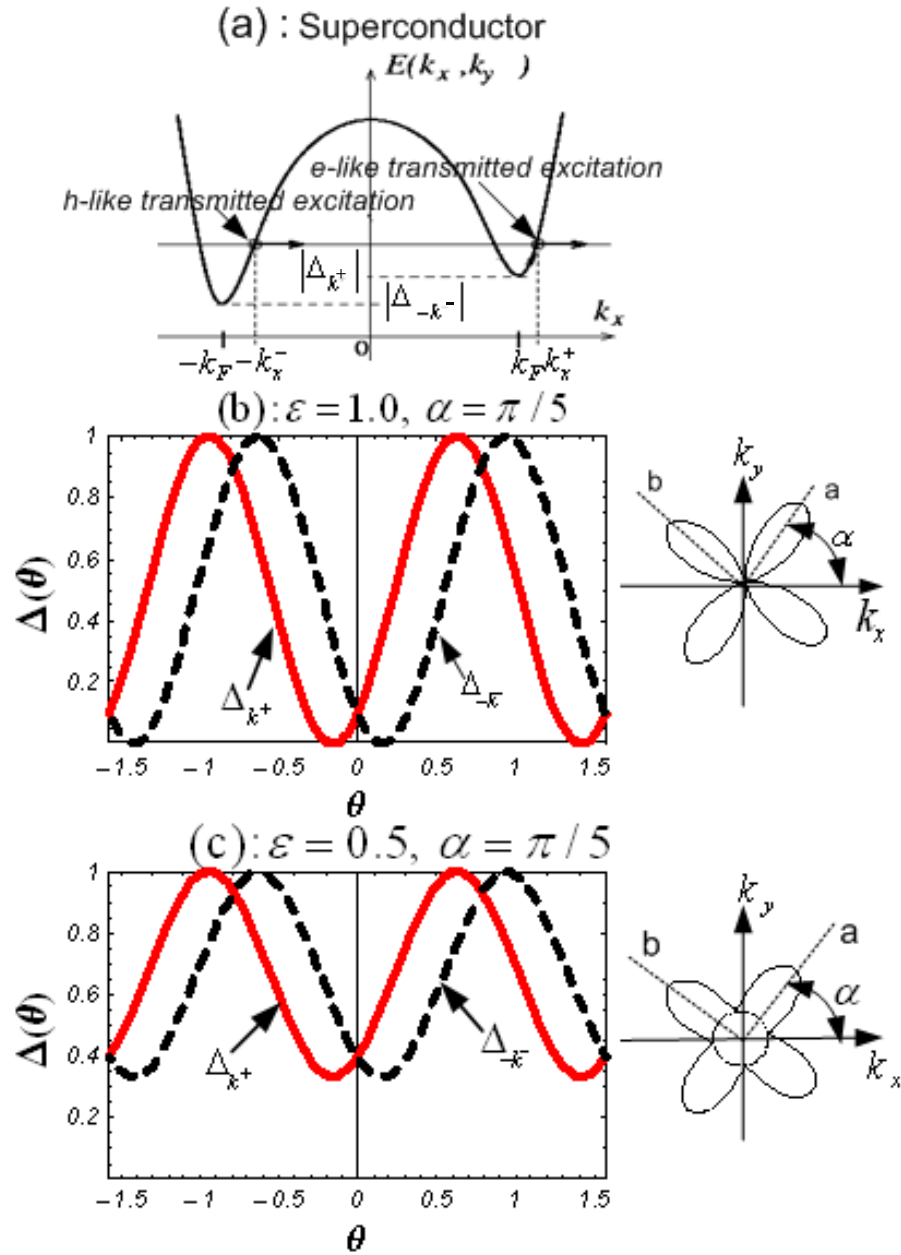


Figure 3.7: (a) The sketch of the excitation energy of the superconductor when  $\alpha \neq 0$ . Note the inequality in  $\Delta_{k^+}$  and  $\Delta_{k^-}$ . The plots of energy gaps as a function of  $\theta$  when orientation angle  $\alpha = \pi/5$  for (b)  $\varepsilon = 1.0$  and (c)  $\varepsilon = 0.5$  are shown. The solid curves are for  $\Delta_{k^+}$  and the dashed curves are for  $\Delta_{-k^-}$ .

The reflection and transmission probabilities as a function of  $E/\Delta_{max}$  with  $\alpha = 0$  and  $Z = 1.0$  at  $\theta = \pi/6$  are shown in Fig. 3.8. In Fig. 3.8(a) the plots are for  $\varepsilon = 1.0$  and in Fig. 3.8(b) they are for  $\varepsilon = 0.5$ . The features of each probability are similar to those in the case of isotropic  $s$ -wave superconductors, only now the main features, such as the peak in  $A$  occurs at  $E = \Delta(\theta = \pi/6)$  instead of at  $E = \Delta_{max}$ . (Note that  $\Delta(\theta = \pi/6)$  is the gap of the excitation that has the momentum making an angle  $\theta = \pi/6$  with the  $x$ -axis).

The plot of each probability is somewhat different in the case when  $\alpha \neq 0$ . Figure 3.9 shows the plots of the reflection and transmission probabilities when  $\alpha = \pi/5$  for both  $\varepsilon = 1.0$  and  $\varepsilon = 0.5$ , and for three different values of  $\theta$ :  $0$ ,  $\pi/4$ , and  $\pi/6$ . For the case where  $\theta = 0$ , the main features, like the peak in  $A$ , of both cases occur at  $E = \Delta(\theta = 0)$  and  $E = \Delta(\theta = \pi/4)$ , respectively. However, for the cases when  $\theta \neq 0$  or  $\theta \neq \pm\pi/4$ , the features in these probabilities are different. For instance, there is no sharp peak in  $A$  any more. There is a plateau, the front edge of which occurs at  $\Delta_{k+} = \Delta(\theta + \alpha)$  while the back edge of which does at  $\Delta_{-k-} = \Delta(\theta - \alpha)$ . It will be seen later on that the sharp peaks in  $A$  for  $\theta = 0$  and  $\theta = \pi/4$  will contribute to the main features in the conductance spectra of the junction of  $\alpha \neq 0$ .

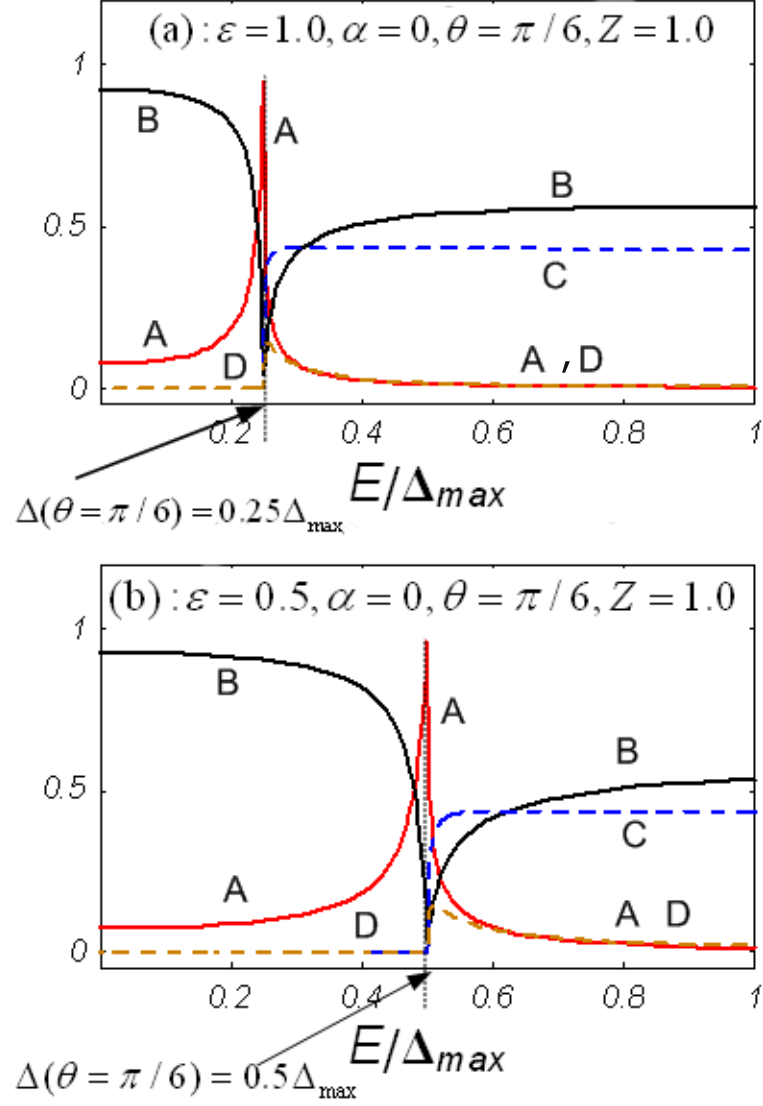


Figure 3.8: The plots of reflection and transmission probabilities of anisotropic  $s$ -wave as functions of  $E$  for  $\theta = \pi/6$ , where  $Z = 1.0$ , and  $\alpha = 0$ . (a) for  $\varepsilon = 1.0$  and (b) for  $\varepsilon = 0.5$ . Note that  $\Delta_{\max} = \Delta_0(1 + |\varepsilon|)$ . A and B are the Andreev and the normal reflection probabilities, respectively. C and D are the transmitted probabilities of e-like and h-like quasiparticle excitations, respectively.

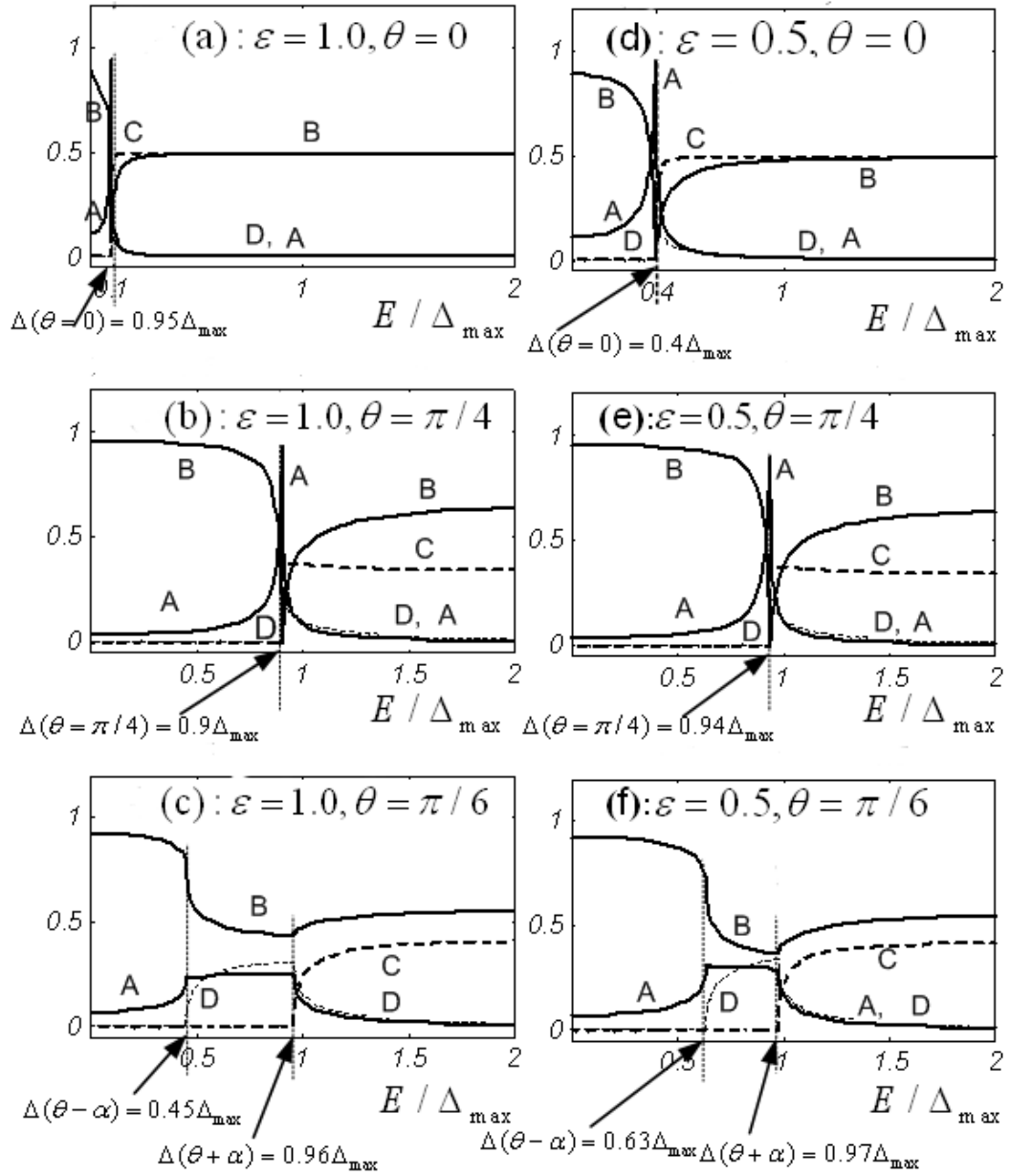


Figure 3.9: The plots of reflection and transmission probabilities as functions of  $E$  when  $Z = 1.0$  and  $\alpha = \pi/5$ . (a), (b), (c) are for  $\epsilon = 1.0$  at  $\theta = 0, \pi/4$ , and  $\pi/6$ , respectively and (d), (e), (f) are for  $\epsilon = 0.5$ , at  $\theta = 0, \pi/4$ , and  $\pi/6$ , respectively.

The normalized conductance of the junction is calculated from Eq.(3.2), which is

$$G(Ve) = \frac{G_{NIS}(Ve)}{G_{NIN}(Ve)} = \frac{\int_{-\pi/2}^{+\pi/2} d\theta \cos\theta \int_{-\infty}^{+\infty} dE T_{NIS}}{\int_{-\pi/2}^{+\pi/2} d\theta \cos\theta T_{NIN}},$$

where  $T_{NIN} = \frac{\cos^2(\theta)}{\cos^2(\theta)+Z^2}$  and  $T_{NIS} = [1 + A(\theta, E) - B(\theta, E)]$ .

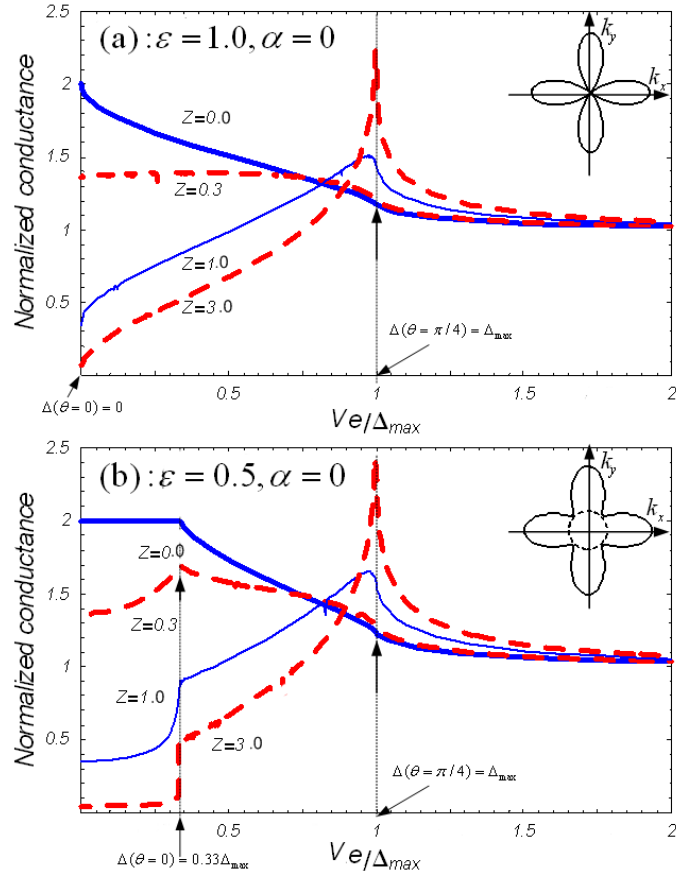


Figure 3.10: The plots of the normalized conductance as a function of  $(Ve)/\Delta_{max}$  at zero temperature for  $\alpha = 0$  with different the values of barrier strength  $Z = 0.0, 0.3, 1.0,$  and  $3.0$ . (a) is when  $\varepsilon = 1.0$ , and (b) is when  $\varepsilon = 0.5$ .

The plots of the normalized conductance as a function of  $(Ve)$  at zero temperature, with  $\alpha = 0$  and different values of  $Z$  are shown in Fig. 3.10. In Fig.

3.10(a), the parameter of the energy gap  $\varepsilon = 1.0$  and in Fig. 3.10(b)  $\varepsilon = 0.5$ . The normalized conductance spectra in both cases have two main features at  $(Ve) = \Delta_{min}$  and  $\Delta_{max}$ .

When  $\alpha \neq 0$ , there are two more features than in the case of  $\alpha = 0$ . These new features occur at  $(Ve) = \Delta(\theta = 0)$  and  $\Delta(\theta = \pi/4)$ , as shown in Fig. 3.11 (which is for the case when  $\alpha = \pi/5$ ). Note that these features are not very apparent when  $Z$  is small. For different  $\alpha$ , the values of  $\Delta(\theta = 0)$  and  $\Delta(\theta = \pi/4)$  are different as well. This means that these features would move when  $\alpha$  is changed.

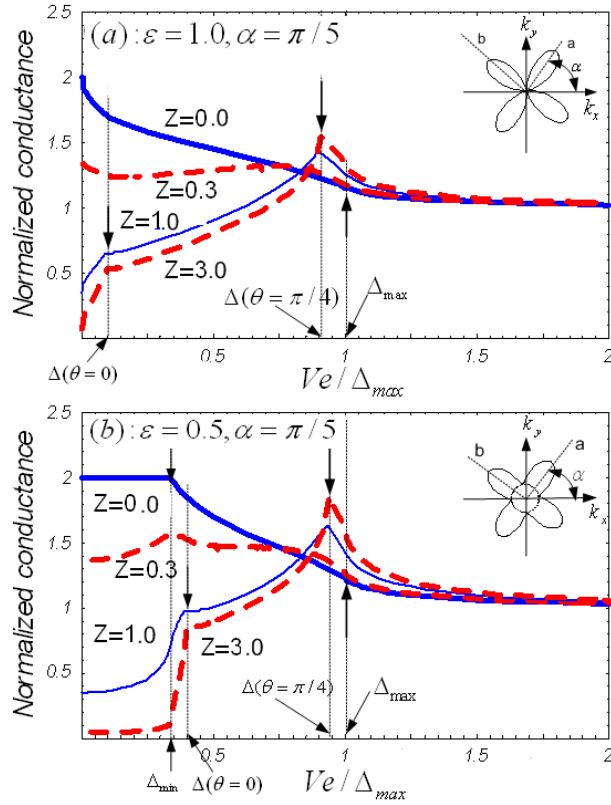


Figure 3.11: The plots of the normalized conductance as a function of  $(Ve)/\Delta_{max}$  with various the value barrier strength  $Z = 0.0, 0.3, 1.0$  and  $3.0$  and orientation by angle  $\alpha = \pi/5$ . (a)  $\varepsilon = 1.0$ , (b)  $\varepsilon = 0.5$ .

Figure 3.12 shows, for the junction with  $Z = 3.0$ , the plots of the normalized



conductance of the junction with different angle  $\alpha$ . Figure 3.12(a) is for when  $\varepsilon = 1.0$  and Fig. 3.12(b) is for when  $\varepsilon = 0.5$ .

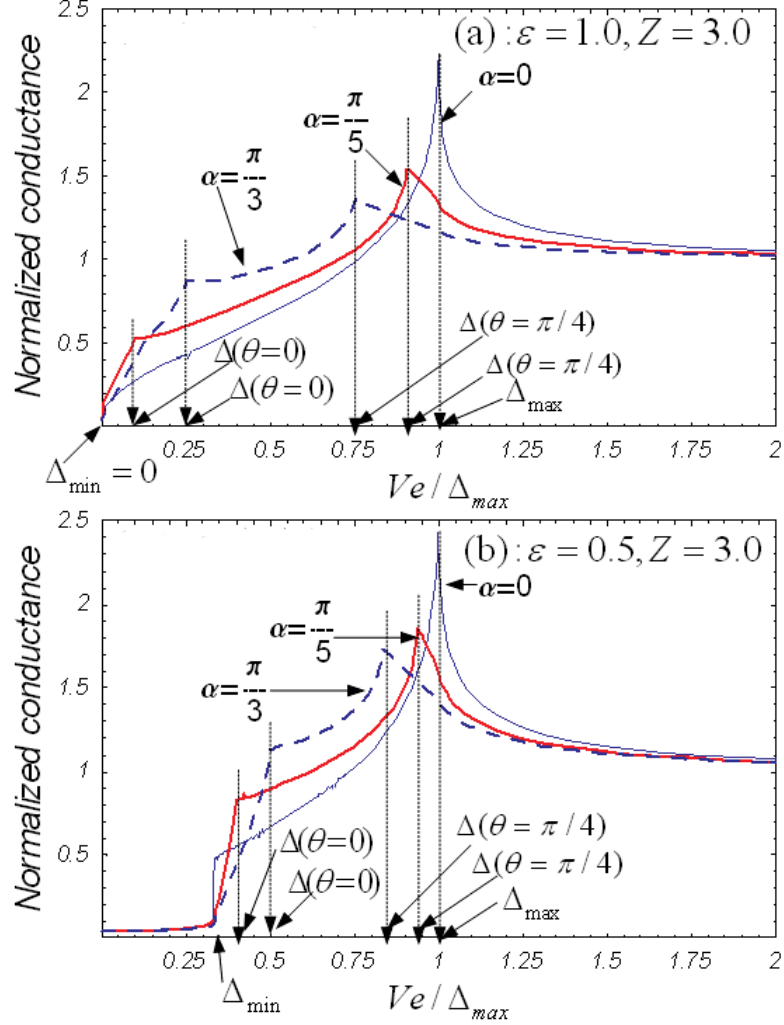


Figure 3.12: The plots of the normalized conductance as a function of  $(Ve)/\Delta_{max}$  with various the value of angle  $\alpha = 0, \pi/5$ , and  $\pi/3$  for  $Z = 3.0$ . (a)  $\varepsilon = 1.0$ , (b)  $\varepsilon = 0.5$ .

The movement of these features with the crystal orientation implies that the NIS tunneling spectroscopy in the tunneling limit can be used to determined the values of the gap function of an anisotropic  $s$ -wave at each point on the Fermi surface.

# Chapter IV

## Tunneling Spectroscopy at Finite Temperatures

### 4.1 Introduction

In this chapter, the effect of finite temperatures on the normalized conductance spectrum is presented. The energy gap of the superconductor is temperature dependent. It can be computed numerically for weak-coupling superconductors. However, at temperatures close to the critical temperature  $T_c$ , the energy gap can be approximated by (Tinkham, M. 1996)

$$\Delta(T) \approx 1.74\Delta \left(1 - \frac{T}{T_c}\right)^{1/2}, \quad T \approx T_c$$

and at temperatures close to the zero temperature, the approximation takes the form (Bardeen, J., *et al.* 1957)

$$|\Delta(T)| \approx |\Delta| \left(1 - \sqrt{\frac{2\pi k_B T}{|\Delta|}} \exp\left[-\frac{|\Delta|}{k_B T}\right]\right), \quad (T \gtrsim 0K).$$

Therefore, the energy gap for of the two transmitted excitations of an anisotropic  $s$ -wave superconductor at temperatures close to zero can be written as

$$\Delta_{k\pm} \approx \Delta(1 + \varepsilon \cos[4(\theta \mp \alpha)]) \left(1 - \sqrt{\frac{2\pi t}{1.76}} \exp\left[-\frac{1}{1.76t}\right]\right),$$

where  $t = T/T_C$ , and  $T_C$  is the critical temperature of the superconductor. In BCS theory,  $\Delta = 1.764k_B T_c$ , which is the magnitude of the energy gap in the bulk of superconductor at zero temperature. As before,  $\varepsilon$  is the parameter of the energy gap,  $\alpha$  is an angle orientation between  $a$ -axis and  $x$ -axis, and  $\theta$  is the angle between the incident electron beam and the  $x$ -axis.  $\Delta_{max}$  is the maximum magnitude of the energy gap in the bulk state of the superconductor.

The normalized conductance formula for calculation at finite temperatures is given by

$$G(Ve, \theta) = \frac{\int_{-\pi/2}^{+\pi/2} d\theta \cos\theta \int_{-\infty}^{+\infty} dE T_{NIS} \frac{\partial}{\partial V} f(E - Ve)}{\int_{-\pi/2}^{+\pi/2} d\theta \cos\theta \int_{-\infty}^{+\infty} dE T_{NIN} \frac{\partial}{\partial V} f(E - Ve)}, \quad (4.1)$$

where  $T_{NIS} = 1 + A(E, \theta) - B(E, \theta)$  and  $A(E, \theta)$  and  $B(E, \theta)$  are respectively the coefficients for the Andreev and normal reflections, which are independent on temperature and  $T_{NIN} = \frac{\cos^2(\theta)}{Z^2 + \cos^2(\theta)}$ .

## 4.2 Isotropic $s$ -wave Superconductor

The normalized conductance of NIS junction is calculated from the Eq.(4.1). Figure 4.1 shows normalized conductance spectra in the case of isotropic  $s$ -wave superconductor at finite temperatures close to zero temperature. All the features in the conductance are smeared out and broadened.

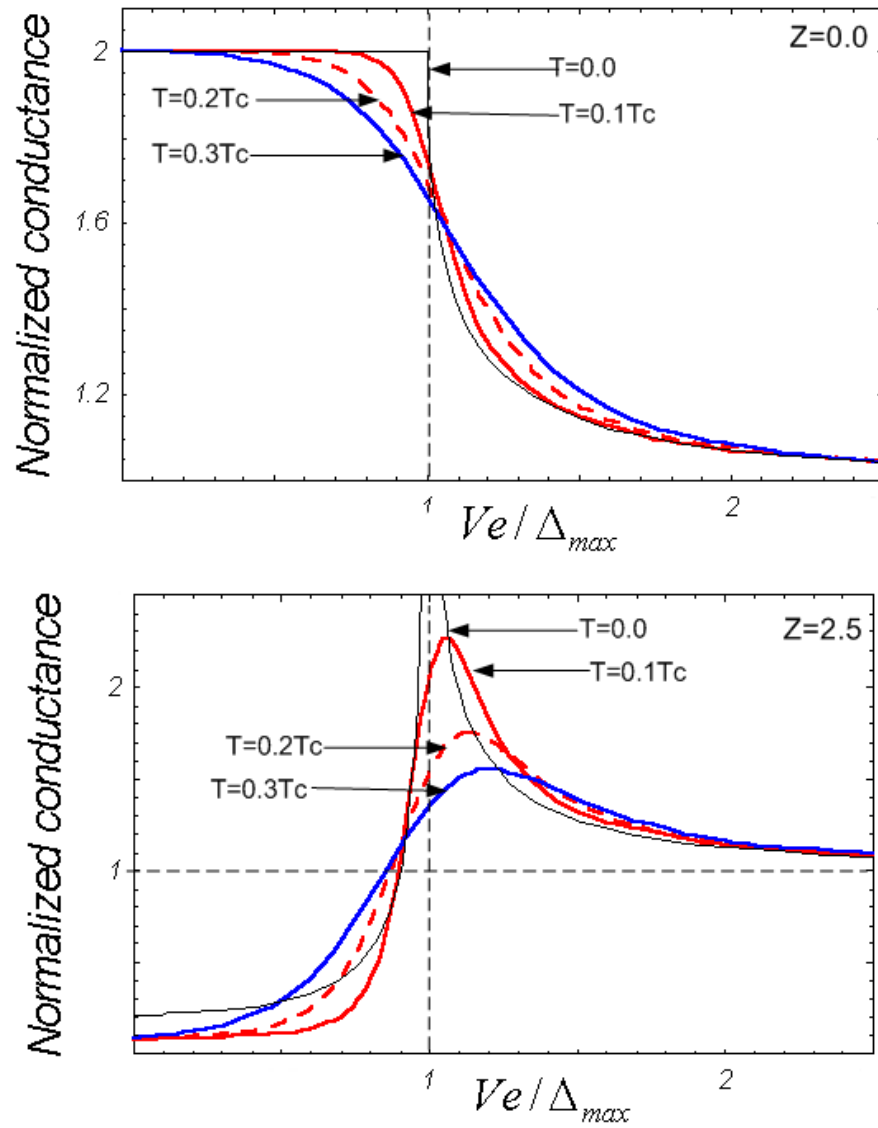


Figure 4.1: The plots of the normalized conductance as a function of  $(Ve)$  at  $T/T_C = 0.0, 0.1, 0.2,$  and  $0.3$ . (a) for  $Z = 0.0$ , and (b) for  $Z = 2.5$ .

### 4.3 Anisotropic $s$ -wave Superconductor

The plots of the normalized conductance as a function of applied voltage in the case where  $Z = 2.5$ , and  $\alpha = 0$  at different temperatures are shown in Fig. 4.2. Figure 4.3 shows the plots of normalized conductance as a function applied voltage where  $\alpha = \pi/6$ , and  $Z = 2.5$  at different temperatures.

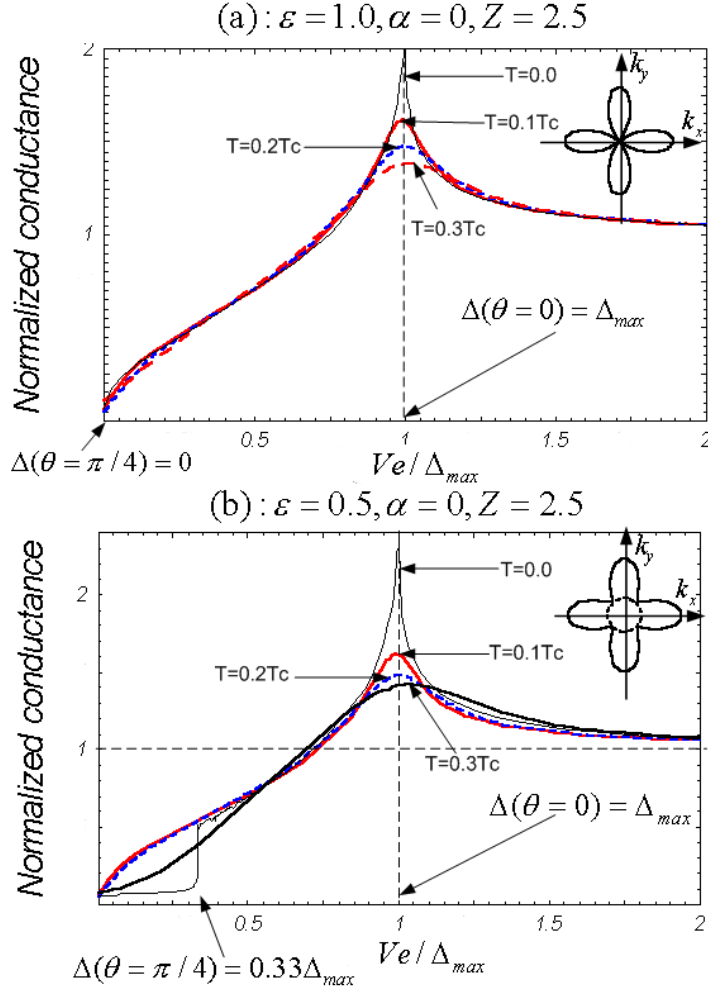


Figure 4.2: The plots of the normalized conductance as a function ( $Ve$ ) at  $T/T_C = 0.0, 0.1, 0.2, 0.3$  and  $\alpha = 0$ , for (a)  $\varepsilon = 1.0$  (b)  $\varepsilon = 0.5$ .

Similar to the case of isotropic  $s$ -wave superconductor, all the features in the conductance spectrum become broader at higher temperatures. The smearing effect caused by finite temperatures suggests that if one wants to use the tunneling

spectroscopy to measure the magnitude of the gap on the Fermi surface, one needs to do the experiment at  $T \lesssim 0.1T_c$ .

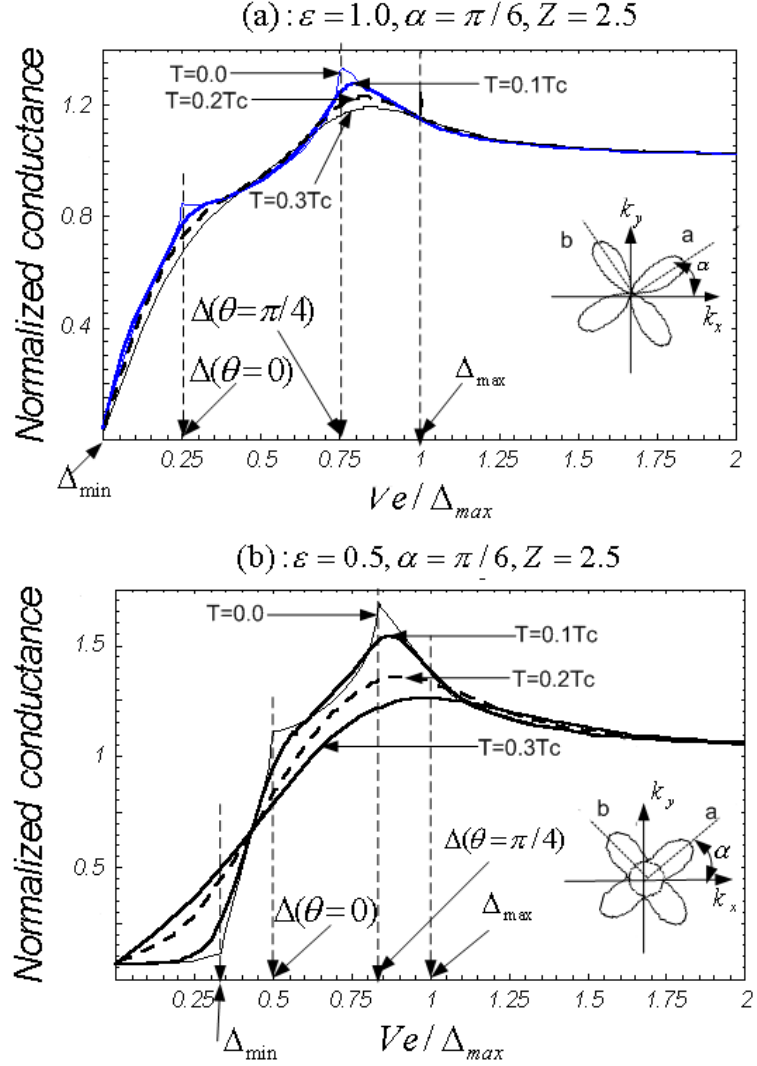


Figure 4.3: The plots of the normalized conductance as a function ( $Ve$ ) at  $T/T_C = 0.0, 0.1, 0.2, 0.3$  and  $\alpha = \pi/6$ , for (a)  $\varepsilon = 1.0$  (b)  $\varepsilon = 0.5$ .

Figure 4.3 shows the plots of normalized conductance as a function  $(Ve)/\Delta_{max}$  when  $\alpha = \pi/6$  and the barrier strength  $Z = 2.5$  for different the temperatures  $T/T_C = 0.0, 0.1, 0.2, 0.3$ , and  $\varepsilon = 1.0$  for Fig.4.3(a),  $\varepsilon = 0.5$  for Fig. 4.3(b). The peaks of the normalized conductance are lowered when the temperature is increased.

# Chapter V

## Conclusions

In this thesis the current and conductance spectra of the normal metal-insulator-anisotropic *s*-wave superconductor junction is studied by using the BTK formalism. This approach makes use of the Bogoliubov-de Gennes equations and the appropriate boundary conditions to calculate the reflection and transmission probabilities as well as the current across the junction. In this approach the dependence on the barrier strength, the interface orientation, and temperature of the tunneling spectroscopy can be examined.

In the high transmission limit, the conductance spectra show that the Andreev reflection dominates at small applied voltage, whereas the normal reflection does in the low transmission limit.

The dependence of the tunneling conductance spectrum on the crystallographic orientation is found to be very useful in determining the magnitude of the energy gap in the momentum space. It is found that there are four distinctive features in the conductance spectra of anisotropic *s*-wave superconductors. These features occur at the voltages corresponding to

- (1) minimum energy gap
- (2) maximum energy gap
- (3) the energy gap of the excitations which have the momentum along the interface normal
- (4) the energy gap of the excitations which have the momentum making the angle  $\pi/4$  with the interface normal.

These features are very distinctive for the junction with low transparency

and at low temperatures. The features found at zero temperature tend to be broadened and smeared out at higher temperatures. Therefore, if one expects to use the tunneling spectroscopy to measure the magnitude of the gap function of anisotropic *s*-wave superconductors, one should do the experiments at low temperatures, at least at the temperatures lower than 10% of the critical temperature.



## References

# References

- Bardeen, J., Cooper, L. N., and Schriffer, J. R. (1957). Theory of Superconductivity. **Phys. Rev.** 108, 1175.
- Blonder, G. E., Tinkham, M., and Klapwijk, T. M. (1982). Transition from metallic to tunneling regimes in superconducting microconstrictions: Excess current, charge imbalance, and supercurrent conversion. **Phys. Rev. B** 25, 4515.
- Buzea, C. and Yamashita, T. (2001). Review of the superconducting properties of  $\text{MgB}_2$ . **Supercond. Sci. Technol.** 14, R115-R146.
- Civale, L., Silhanek, A. V., Thompson, J. R., Song, K. J., Tomy, C. V., and Paul, D. M. (1999). Fourfold basal plane anisotropy of the nonsocial magnetization of  $\text{YNi}_2\text{B}_2\text{C}$ . **Phys. Rev. Lett.** 83, 3920.
- Demers, J. and Griffin, A. (1971). 285 Scattering and tunneling of electronic excitations in the Intermediate state of superconductors. **Canadian Journal of Physics** 49, 285.
- Duzer, T. V. and Turner, C. W. (1999). **Principles of superconductive devices and circuits.** (2nd ed.). Prentice-Hall, Inc. A Simon and Schuster Company.
- Giaver, I. (1960). Energy gap in superconductors measured by electron tunneling. **Phys. Rev. Lett.** 5, 147.
- Giaver, I. and Megerle, K. (1961). Study of superconductors by electron tunneling. **Phys. Rev.** 122, 1101.

- Griffin, A. and Demers, J. (1971). Tunneling in the normal-metal-insulator-superconductor geometry using the Bogoliubov equation of motion. **Phys. Rev. B** 4, 2202.
- Kashiwaya, S., Tanaka, Y., Koyanagi, M., and Kajimura, K. (1996). Theory for tunneling spectroscopy of anisotropic superconductors. **Phys. Rev. B** 53, 2667.
- Maki, K., Thalmeier, P., and Won, H. (2002). Anisotropic *s*-wave superconductivity in borocarbides  $\text{LuNi}_2\text{B}_2\text{C}$  and  $\text{YNi}_2\text{B}_2\text{C}$ . **Phys. Rev. B** 65, 140502.
- McMillan, W. L. and Rowell, J. M. (1969). **Superconductivity**. edited by Parks R. D. (Marcel-Dekker, New York), Vol. 1, p. 561.
- Mortensen, N. A., Flensberg K., and Jauho, A-P. (1999). Angle dependence of Andreev scattering at semiconductor-superconductor interfaces. **Phys. Rev. B** 59, 10176.
- Mun, M-O., Lee, S-l., and Choi, B. K. (1998). Magnetic field effect on the transport properties of quaternary inter metallic superconductor  $\text{YNi}_2\text{B}_2\text{C}$ . **Chinese Journal of Physics** 36, 324.
- Nohara, M., Isshiki, M., Takagi, H., and Cava, R. J. (1997). Magnetic Field Dependence of Low-Temperature Specific Heat of the Borocarbide Superconductor  $\text{LuNi}_2\text{B}_2\text{C}$ . **Journal of the Physical Society of Japan** Vol. 66, No 7, pp. 1888-1891.
- Pairor, P. and Walker, M. B. (2002). Tunneling Conductance for *d*-Wave Superconductor: Its Dependence on Crystallographic Orientation and Fermi Surface. **Phys. Rev. B** 65, 064507.
- Pickett, W. E. and Singh, D. J. (1994).  $\text{LuNi}_2\text{B}_2\text{C}$ : A Novel Ni-Based strong-coupling superconductor. **Phys. Rev. Lett.** 72, 3702.

- Shulga, S. V., Drechsler, S-L., Fuchs, G., and Müller, K-H. (1998). Upper Critical Field Peculiarities of Superconducting  $\text{YNi}_2\text{B}_2\text{C}$  and  $\text{LuNi}_2\text{B}_2\text{C}$ . **Phys. Rev. Lett.** 80, 1730.
- Song, K. J., Thompson, J. R., Yethiraj, M., and Christen, D. K. (1999-II). Non-local current-field relation and the vortex-state magnetic properties of  $\text{YNi}_2\text{B}_2\text{C}$ . **Phys. Rev. B** 59, R6620.
- Tinkham, M. (1996). **Introduction to superconductivity**. (2nd ed.). McGraw-Hill, Inc..
- Wolf, E. L. (1985). **Principle of electron tunneling spectroscopy**. Oxford University Press, NewYork.
- Zarestky, J., Stassis, C., Goldman and Canfield, P. (1999). Phonon profile in superconducting  $\text{LuNi}_2\text{B}_2\text{C}$  and  $\text{YNi}_2\text{B}_2\text{C}$ . **Phys. Rev. B** 60, 11932.

## Curriculum Vitae

Mr. Sonesacksith Bounma was born on 02 January 1962 in Xaythanee District, Vientiane Municipality, Lao People Democratic Socialist Republic. In October 1983, he went to study in the Department of Physics, Institute of Science at No.I Hanoi University Socialist Republic Vietnam, and graduated in July 1989. From October 1989 to November 1996, he worked as a teacher of Physics in Preparatory School for Student to Studies Abroad in Vientiane. After that, he was a teacher of Physics at School of Foundation Study in the National University of Laos until February 2000. In March 2000, he came to study in a Master's degree of Physics program at Institute of Science, Suranaree University of Technology.